

INTRODUCTION TO QUANTUM CHAOS

Denis Ullmo¹ and Steven Tomsovic²

¹*LPTMS, Univ Paris-Sud, CNRS UMR 8626, 91405
Orsay Cedex, France*

²*Department of Physics and Astronomy, Washington State University,
Pullman, WA 99164-2814 USA*

July 17, 2014

Keywords: quantum chaos, random matrix theory, spectral statistics, Gutzwiller trace formula, periodic orbit theory, kicked rotor, diamagnetic hydrogen, Coulomb blockade, orbital magnetism.

Contents

1	Introduction	3
2	Background context and history	4
2.1	Chaos	4
2.2	Quantum Mechanics	6
2.3	Correspondence Principle & Quantum Chaos	7
3	The kicked rotor	8
3.1	The classical rotor	9
3.2	The quantum rotor	9
3.3	Classical emergence	12
4	Semiclassical description of chaotic systems	12
4.1	Bohr-Sommerfeld quantization rule	13
4.2	Gutzwiller trace formula	14
4.3	Orbit proliferation and convergence issues	14
4.4	Breaking the mean level spacing scale	15
5	Random Matrix Theory	17
5.1	Spectral statistics	18
5.2	Random Matrix Ensembles	19
5.3	Quantum chaos and Random matrices	21
6	Physical applications	23
6.1	The Hydrogen atom in a strong magnetic field	24
6.2	Coulomb Blockade in a ballistic quantum dot	28
6.3	Orbital magnetism of mesoscopic rings or dots	30
7	Conclusion	32

Summary

The authors provide a pedagogical review of the subject of Quantum Chaos. The subject's origins date to the debut of the twentieth century when it was realized by Einstein that Bohr's Old Quantum Theory could not apply to chaotic systems. A century later, the issues arising in trying to understand the quantum mechanics of chaotic systems are actively under research. The main theoretical tools for exploring how chaos enters into quantum mechanics and other wave mechanics such as optics and acoustics, are semiclassical methods and random matrix theory. Both are briefly reviewed in their own chapters. The kicked rotor, an important simple paradigm of chaos, is used to illustrate some of the main issues in the field. The article proceeds with applications of quantum chaos research to understanding the results of three very different experimental systems.

1 Introduction

It is not trivial to compose a concise statement that defines the meaning of quantum chaos precisely. In fact, it may be more helpful to begin with a description. One branch of quantum chaos encompasses a statistical mechanics based on the nature of a system's dynamics, be it chaotic, diffusive, integrable, or some mixture. This means that one is not relying on the thermodynamic limit in which the number of particles tends to infinity. Another branch is an analysis of what the behaviors of linear wave equation solutions may be in a short wavelength or asymptotic limit. It applies equally well in the contexts of quantum mechanics, acoustics, optics, or other linear wave systems, and quantum chaos is sometimes referred to as wave chaos, which is really the more general moniker. As the subject has developed, these two branches have become intimately intertwined with each other and with parts of the theory of disordered systems. From investigations of quantum chaos, many unexpected and deep connections have emerged between quantum and classical mechanics, and wave and ray mechanics as well as newly identified asymptotic and statistical behaviors of wave systems. Hopefully, the meaning of these somewhat abstract statements will develop into a clearer mental image as you proceed through the general subject introduction provided here.

The study of quantum chaos has multiple, important motivations. First, it is absolutely essential if one wishes to understand deeply the interface between the quantum and classical mechanical worlds. Together they form the foundation for all of physics and there is still much left to uncover about their connections and the Correspondence Principle. In addition, quantum chaos has pushed the development of new theoretical techniques and methods of analysis that apply to a wide variety of systems from simple single particle systems to strongly interacting many-body systems to branches of mathematics. These developments are still underway and are still being applied to new domains.

A fascinating feature of quantum chaos is that it reveals a significant amount of *universality* in the behavior of extraordinarily different physical systems. For example, acoustic wave intensities found in problems with strong multiple scattering that lead to a probability density known as the Rayleigh distribution, Ericson fluctuations in the cross-sections of neutrons scattering from medium to heavy nuclei, and conductance fluctuations found in chaotic or disordered quantum dots can be seen to possess a common underlying statistical structure. One is thus able to see essential parallels between systems that would normally otherwise be left uncovered. Universality implies a lack of sensitivity to many aspects of a system in its statistical properties, i.e. an absence of certain kinds of information. Furthermore, quantum chaos brings together many disparate, seemingly unrelated concepts, i.e. classical chaos, semiclassical physics and asymptotic methods, random matrix ensembles, path integrals, quantum field theories, Anderson localization, and ties them together in unexpected ways. We cannot cover all of these topics here, and so make a selection of important foundations to cover instead. However, we will list a few references at the end to some of what has been left out for the interested reader.

It is not surprising then to see that quantum chaos has found application in many domains. A partial list includes: i) low energy proton and neutron resonances in medium and heavy nuclei; ii) ballistic quantum dots; iii) mesoscopic disordered electronic conductors; iv) the Dirac spectrum in non-Abelian gauge field backgrounds; v) atomic and molecular spectra; vi) Rydberg atoms and molecules; vii) microwave-driven atoms; viii) ultra-cold atoms and optical lattices; ix) optical resonators; x) acoustics in crystals and over long ranges of propagation in the ocean; xi) quantum computation and information studies; xii) the Riemann zeta function and generalized L-functions; and xiii) decoherence and fidelity studies. There are many other examples.

The structure of this contribution is the following. The next section covers critical back-

ground and historical developments. This is followed by the introduction of a historically important, simple dynamical system, the kicked rotor, which illustrates the notion of the quantum-classical correspondence, and provides in this way some intuition of why, and in what way, one should expect classically chaotic dynamics to influence the quantum mechanical properties of a system. Section 4 goes into the more formal aspects of the quantum-classical correspondence, and in particular gives a more concrete sense to different approximation schemes going under the name of *semiclassical approximations*. It covers a brief review of the Bohr (or more generally Einstein-Brillouin-Keller) quantization scheme, and discusses why this approach can be applied only to integrable systems. This is followed by a description of *semiclassical trace formulae*, applicable for a much wider range of dynamics, and in particular of the *Gutzwiller trace formula* valid in the chaotic regime. Section 5 introduces random matrix theory, which has proven extremely fruitful in the context of the quantum dynamics of classically chaotic systems, namely the statistical description of the spectrum and eigenfunctions. Finally, in Sect. 6 we select a few systems, or problems, for which the concepts of quantum chaos have proven useful. We will in particular show how the tools described in Sects. 4 and 5 can be applied in different physical contexts by considering the examples of the Hydrogen atom in a strong magnetic field, the Coulomb Blockade in ballistic quantum dots, as well as some aspects of orbital magnetism.

2 Background context and history

2.1 Chaos

At the end of the nineteenth century, the paradigm most physicists (as well as most everyone actually) were relying on to understand the physical world was derived from the motion of planets. Within this paradigm, physical objects could be described by their position and velocity, quantities which could be known arbitrarily well or at least as precisely as one was able to measure them. Their time evolution was governed by Newton's laws, which form a completely deterministic set of equations, and the subject is known as classical mechanics. However, exact solutions of these equations were derived only in certain simple cases, and it was usually assumed that sophisticated approximation schemes could provide arbitrarily accurate solutions – as long as one was willing to put enough effort into the calculations.

A limitation to this notion that, at least in principle, it is possible to have complete predictive power with respect to the dynamics of physical objects, arose with the realization that the solutions to Newton's equations could be exponentially unstable. Already, Poincaré, in his study of the “three-body problem” of celestial dynamics knew that under many circumstances, a qualitatively different and significantly more complex kind of dynamics was taking place now known as chaos. It is worth understanding how it differs from the dynamics of more readily solvable systems.

Let us begin by considering a stable, effectively one body, dynamical system, the Earth revolving around the Sun at position \mathbf{r} and with a momentum \mathbf{p} relative to the Sun. Assuming the Sun's mass is immensely greater than the Earth's, the Earth's motion is governed by the classical Hamiltonian (the total energy of the system - kinetic plus potential)

$$H_{\text{cl}} = \frac{\mathbf{p}^2}{2M_{\oplus}} + V(\mathbf{r}) , \quad (1)$$

associated with the gravitational potential energy

$$V(\mathbf{r}) = -\frac{GM_{\odot}M_{\oplus}}{|\mathbf{r}|} , \quad (2)$$

where $\{M_{\oplus}, M_{\odot}\}$ are the Earth's and Sun's masses, respectively, and G is the gravitational constant. The derivative changes in position and momentum $\dot{\mathbf{r}}$ and $\dot{\mathbf{p}}$ are given by Hamilton's equations

$$\begin{aligned}\dot{\mathbf{r}} &= +\frac{\partial H_{\text{cl}}}{\partial \mathbf{p}} = \frac{\mathbf{p}}{M_{\odot}} \\ \dot{\mathbf{p}} &= -\frac{\partial H_{\text{cl}}}{\partial \mathbf{r}} = -\frac{\partial V}{\partial \mathbf{r}},\end{aligned}\tag{3}$$

which can be shown to be equivalent to the Newton equations of motion $M_{\oplus}\ddot{\mathbf{r}} = -\partial V/\partial \mathbf{r}$. Depending on the initial conditions, $(\mathbf{r}(0), \mathbf{p}(0))$, Eq. (3) is solved with Eqs. (1,2) to give the known (Keplerian) elliptical orbits that are excellent approximations to Earth's true motion.

It turns out that both the kinetic energy term $\mathbf{p}^2/2M_{\oplus}$ and the gravitational potential $V(\mathbf{r})$ are invariant under a rotation of the physical space. This implies that one can construct two independent constants of the motion associated with angular momentum. Adding another to this list, Earth's total energy, which is conserved because the Hamiltonian, Eqs. (1,2), has no explicit time dependence, there are three constants of the motion. Any system, such as this, which has as many constants of motion as degrees of freedom is said to be *integrable*. Integrability implies that the motion of the system is stable in the sense that a small change in the initial position or velocity implies a small change, with a linear time-dependence of the final position and velocity. In the same way, a small perturbation of an integrable Hamiltonian, as could be realized by accounting for Jupiter's gravitational pull on the Earth, would not drastically alter the trajectories or stabilities.

Before modern computers made it possible to perform extensive numerical simulations, the class of problems physicists or mathematicians could effectively solve were either integrable or sufficiently near integrability that a perturbative scheme could be applied. This class included both the “two-body problem”, i.e. two bodies interacting via a central force such as the Earth example, and small perturbations around stable equilibrium points. The theory was very successful for this broad range of physical situations, and at times it was erroneously assumed that to broaden the range of treatable problems, one had merely to work harder doing longer calculations or calculate more terms in a perturbations series.

However, integrability and/or near-integrability is a rather exceptional property for a dynamical system to possess. Systems with three or more bodies interacting often behave radically different from integrable systems. The motion of Earth's Moon or Pluto are both chaotic as each are effectively part of a three body system (Sun, Earth, Moon or Sun, Neptune, Pluto). Even deceptively simple looking systems may display chaos. Consider Bunimovich's stadium billiard, mathematically proven completely chaotic, shown in Fig. 1, and consider a point-like particle of mass m moving freely (that is in a straight line) inside the billiard and subject to specular reflection on the boundaries. Contrary to the Earth's orbit around the Sun, a particle's motion within this billiard is highly unstable. As illustrated in Fig. 1, two trajectories initiated with slightly different initial conditions diverge exponentially quickly from each other, and after just a few bounces are not correlated anymore. In the same way, even the slightest perturbation would completely change a trajectory after a relatively small number of bounces. The motion within the stadium billiard is associated with the strongest form of chaotic dynamics. It is perfectly deterministic, so that exact knowledge of position and velocity at some initial time fixes the evolution to all times, and yet the evolution is so unstable that any uncertainty in the initial conditions quickly makes both position and velocity unpredictable.

After the pioneering work of Poincaré, little progress was made in the study of chaotic systems and, more generally, of systems far from integrability until the 1960's or 1970's. Then computer simulations made it possible to develop one's intuition about their behaviors and to motivate more formal work concerning their qualitative and statistical properties. Note that

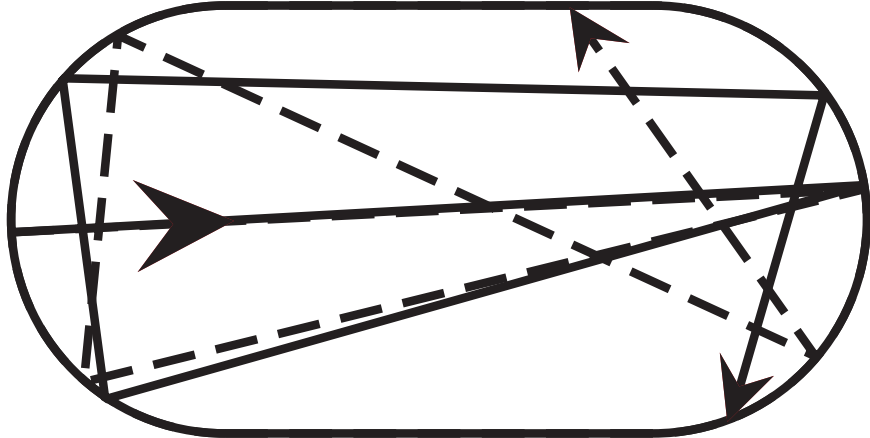


Figure 1: An example of a strongly chaotic system: the Bunimovich stadium billiard. The two trajectories indicated by the solid and dashed lines begin with a slightly different starting point. Their divergence is an illustration of exponential sensitivity to initial conditions.

integrable and chaotic systems correspond to the two limiting cases of the most stable and most unstable dynamics. Typical low dimensional systems usually fall in the intermediate category of *mixed dynamics* in which integrable-like and chaotic-like motions coexist in different regions of phase space.

2.2 Quantum Mechanics

A second, quite fundamental limitation to the notion that one could have complete predictive power over physical objects, arose with the realization that microscopic systems, such as atoms and molecules require a description in terms of quantum mechanics. Classically and non-relativistically, the Hydrogen atom, other than the values of its constants and microscopic size, leads to equations identical to that of the Sun and Earth system; i.e.

$$H_{\text{cl}} = \frac{\mathbf{p}^2}{2m_e} + V(\mathbf{r}) \quad (4)$$

with

$$V(\mathbf{r}) = -\frac{e^2}{4\pi\epsilon_0|\mathbf{r}|}, \quad (5)$$

where m_e is the mass of the electron, e the electric charge, and ϵ_0 the permittivity constant. The electron then in a classical world would follow elliptical orbits around the proton in a Hydrogen atom just like the Earth moves around the Sun.

Quantum mechanics implies however drastic conceptual changes. Rather than being entirely characterized by it's position and velocity, the electron is now described by a wave-function $\psi(\mathbf{r}, t)$, whose modulus square $|\psi(\mathbf{r}, t)|^2$ specifies the probability that the particle can be found at position \mathbf{r} at time t . As a consequence position, as well as velocity, can be known only in a probabilistic way, not with an arbitrary precision, and not simultaneously. The time evolution of the wavefunction is then given by the [time-dependent] Schrödinger equation

$$i\hbar\frac{\partial\psi}{\partial t} = \hat{H}_{\text{qu}}\psi, \quad (6)$$

where the quantum version of the Hamiltonian

$$\hat{H}_{\text{qu}} \stackrel{\text{def}}{=} -\frac{\hbar^2}{2m_e}\Delta + V(\mathbf{r}) \quad (7)$$

is obtained from the classical counterpart H_{cl} Eq. (4) through the substitution $\mathbf{p} \rightarrow -i\hbar\nabla_{\mathbf{r}}$.

From the Schrödinger equation, Eq. (6), we see that in quantum mechanics a particular role will be played by the static solutions, called eigenenergies and eigenfunctions, of the quantum Hamiltonian \hat{H}_{qu} , i.e. the set of real numbers ϵ_n and functions $\varphi_n(\mathbf{r})$ ($n = 0, 1, 2, \dots$) fulfilling the eigenvalue equation (or stationary Schrödinger equation)

$$\hat{H}_{\text{qu}}\varphi_n = \epsilon_n\varphi_n . \quad (8)$$

Indeed, from Eq. (6) the time evolution of the n 'th eigenfunction is $\varphi_n(t) = \varphi_n(0) \exp[-i\epsilon_n t/\hbar]$. Therefore to within the phase $\exp[-i\epsilon_n t/\hbar]$, which is not a measurable quantity, φ_n is a stationary function. In a more rigorous theory of the Hydrogen atom, in which the interaction with the electromagnetic environment is included, the energies $\hbar\omega$ of the photons emitted or absorbed by the atom are generally given by the difference $(\epsilon_n - \epsilon_{n'})$ between two eigenenergies. This indicates that the Hydrogen atom has switched from the state φ_n to the state $\varphi_{n'}$. As the most natural way to probe the properties of an atom or a molecule is to look at the color of the light they emit or absorb, i.e. at the energy of the corresponding photons, the spectrum of an atom or molecule (that is the set of all energies of the corresponding quantum Hamiltonian) is the most immediate quantity to access. In addition, many important properties of quantum systems, and in particular thermodynamic quantities, are entirely determined by their energy spectra. More focus ahead is on the description of the quantum energy spectra, keeping in mind however that this does not exhaust the richness of the quantum world.

2.3 Correspondence Principle & Quantum Chaos

In the early twentieth century quantum mechanics began with a primitive form known as the “Old Quantum Theory.” It was the statement that among all possible trajectories, only one with the classical action $J \stackrel{\text{def}}{=} \oint \mathbf{p} d\mathbf{r}$ being a multiple of Planck’s constant $2\pi\hbar$ could actually correspond to a stationary state of the quantum particle. The action, and thus the energy of the electron had to be “quantized”.

In the modern form of quantum mechanics the link between the quantum and the classical world is less immediate, but still exists through what is referred to as the Correspondence Principle. For instance, the quantum Hamiltonian Eq. (7) describing the Hydrogen atom could be associated with a classical counterpart, here given by Eqs. (1)-(5). This remains true on a very general basis. Quantum Hamiltonians can be associated with a classical analog, which, in some sense corresponds to its classical limit as $\hbar \rightarrow 0$ (or more correctly when all action variables are large compared with \hbar).

Even before the emergence of the full quantum theory, it was recognized that the primitive form can only apply to integrable systems. With the modern form of quantum mechanics, the Correspondence Principle is effective irrespectively of the nature of the dynamics. A question that naturally arises then is whether this concept of chaos, which has been developed in the context of classical physics, is relevant when studying a quantum system.

This interrogation could actually be approached in two rather different ways. The first one would be to decide whether, for instance, by making a choice different than Eq. (5) of the potential $V(\mathbf{r})$, there exists a class of quantum Hamiltonians such that the Schrödinger equation (6) is chaotic. One possible sense of the term “chaos” here could be that two slightly different initial wave functions $\varphi_1(\mathbf{r}, t = 0)$ and $\varphi_2(\mathbf{r}, t = 0)$ diverge “exponentially” rapidly from one another with time. It turns out however that one can answer this question under relatively general conditions, and the answer is negative. Indeed, the simple fact that the Schrödinger equation is linear (i.e. that a linear combination of two solutions of Eq. (6) is also a solution of this equation) makes it impossible that chaos, in any sense similar to classical mechanics, develops in quantum mechanics.

Another more interesting and productive approach to the role of chaos in quantum mechanics is associated with exploring the interrelations mentioned above between a quantum system and its classical analog through the Correspondence Principle. Indeed, within this framework it becomes meaningful to ask whether the quantum mechanics of some system is qualitatively different if its classical analog displays a completely chaotic and irregular behavior. The answer to this question is positive, and one purpose of *quantum chaos* is to determine in what ways. We shall illustrate this statement in the next section using the particular example of the kicked rotor, and come back after that to a discussion of the role of chaos in quantum mechanics with a broader perspective.

3 The kicked rotor

For the past fifty years the kicked rotor has provided an extraordinary paradigm that has been instrumental in the theoretical development of quantum chaos. From a classical perspective alone, the rotor is a natural paradigm for many reasons. Its form is well motivated by generalized coordinate systems essential for understanding the dynamics of integrable systems called action-angle variables. In these coordinates, integrable dynamics is like free particle dynamics in a phase space that is cylindrical (the position coordinate is an angle). Perhaps the simplest, non-trivial perturbation imaginable is to tap the system repetitively with a potential which is periodic in the angular variable. The lowest term in a frequency decomposition would be a single sinusoidal term. So first, the kicked rotor serves as a paradigm for how perturbations destroy integrability and near-integrable dynamics in general. It has been extremely valuable in studies related to the Kolmogorov, Arnol'd, Moser (KAM) theory about how the quasi-periodic motion of integrable systems survives or is destroyed by perturbation. It has a control parameter whose value determines the nature of the dynamics. For small values, the system is integrable or nearly so, and as it increases the system transitions toward a more fully developed, completely and strongly chaotic dynamics. Furthermore, there are two main versions of great utility. The first version has the phase space of an infinite cylinder. Its dynamics in the momentum variable exhibits a range of behaviors from a contained dynamics for the integrable and near-integrable regime to diffusive in the fully chaotic regime. In between, it displays combinations of diffusion, confined dynamics, and accelerator modes, which rapidly increase their energies. Its diffusion constants, action diffusion constants, and Lyapunov exponents (measuring its exponential instability) can be calculated analytically and other quantities such as the parameter value of the last KAM torus break-up have been studied extensively. The second version is periodic in momentum, similar to position. The phase space is a so-called torus, which is compact (or finite in its extent). There the dynamics can range from integrable to chaotic, but diffusion in momentum is no longer possible. It is more useful as a paradigm for bounded systems, whereas the former is more useful for open systems.

Quantum mechanically, the kicked rotor's quantization on a cylinder is straightforward and well adapted for efficient numerical studies. It has been mapped onto a Lloyd model of Anderson localization (assuming pseudo-random numbers can represent truly random numbers) and its eigenfunctions' localization properties have been studied extensively and in many regimes. There is also a reflection symmetry about zero momentum that enables one to study a novel form of quantum tunneling between Anderson localized eigenstates. It has been instrumental in studies of quantum suppression of classical diffusion, quantum accelerator modes, and more recently, studies of the fidelity. It has also played an important role in the understanding of the statistical nature of extreme values of the eigenangles and eigenvectors, and how their statistics influence quantum entanglement and quantum information theory.

3.1 The classical rotor

A general kicked rotor is a mechanical-type particle constrained to move on a ring that is kicked instantaneously every multiple of a unit time, $t = n\tau$. Supposing the radius of the ring to be $1/2\pi$ and $\tau = 1$, the Hamiltonian takes the form

$$H(x, p) = \frac{p^2}{2} + V(x) \sum_{n=-\infty}^{\infty} \delta(t - n), \quad (9)$$

where $V(x)$ is a function periodic on the interval $x \in [0, 1]$. From $H(x, p)$, mapping equations relating the position and momentum (x_{i+1}, p_{i+1}) of the particle just before the $(n+1)$ 'th kick to the one (x_i, p_i) just before the n 'th kick are obtained as

$$\begin{aligned} p_{n+1} &= p_n - V'(x_n) \\ x_{n+1} &= x_n + p_{n+1}. \end{aligned} \quad (10)$$

The notation V' indicates the derivative of V with respect to x . The simplest periodic function on a ring is just the lowest harmonic

$$V(x) = -\frac{K}{4\pi^2} \cos(2\pi x) \quad (11)$$

and leads to the standard map.

Figure 2 shows the transition from integrable (regular) dynamics to chaotic dynamics as K increases. At $K = 0$ the map is integrable and is essentially a stroboscopic map of a freely rotating particle. There are both rational and irrational tori, depending on whether the frequency of rotation is commensurate or not with the frequency of the strobe. As the kicking strength is increased from zero with exactly the same frequency of stroboscopic observation, the incommensurate tori (irrational) survive small perturbations in accordance with the KAM theorem, while the commensurate (rational) ones break up into a pair of stable and unstable orbits in accordance with the Poincaré-Birkhoff theorem. The phase space becomes mixed with stable and chaotic orbits for increasing K . At around $K \approx 1$ the last rotational irrational KAM tori breaks and this leads to global diffusion. Up to $K = 4$ a stable fixed point persists. Beyond $K \approx 5$ the standard map is considered to be largely chaotic, although it is also not proven to be completely chaotic for any value of K . At an infinity of values of K stable fixed points are known to appear in the $p = 0$ line for the map on the torus that are accelerator modes for the map on the cylinder. These typically occupy regions in the phase space whose areas scale as $1/K^2$. The Lyapunov exponent of the map, which measures the rate of divergence of nearby chaotic trajectories, increases as $\ln(K/2)$ (to a very good approximation for large K).

3.2 The quantum rotor

The quantized version of the standard map relies on the single time step propagator \hat{U} which relates the quantum wave function of the rotor $\varphi(x; t=n)$ just before the n 'th kick to the one $\varphi(x; t=(n+1))$ just before the $(n+1)$ 'th kick

$$\varphi(x; t=(n+1)) = \hat{U}\varphi(x; t=n). \quad (12)$$

The operator \hat{U} is therefore the closest quantum analog to the classical mapping Eq. (10).

The position variable can take on only quantized values and forms a complete basis for the quantization. In this discrete basis the propagator is an $M \times M$ matrix given by

$$\langle m | \hat{U} | m' \rangle = \frac{1}{\sqrt{iM}} \exp(i\pi(m-m')^2/M) \exp\left(i\frac{KM}{2\pi} \cos(2\pi(m+1/2)/M)\right). \quad (13)$$

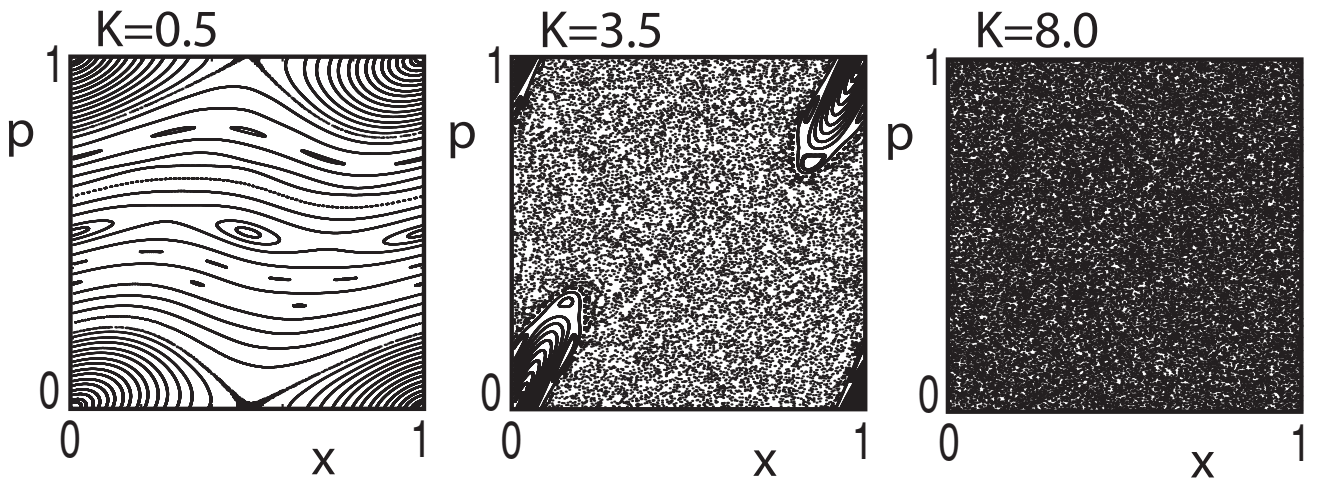


Figure 2: Three Poincaré surfaces of section obtained for different values of the coupling K by iterating the map Eqs. (10,11) for one ($K = 8.0$) or a few ($K = 0.5$ and $K = 3.5$) initial conditions. The left section illustrates nearly integrable dynamics. The break up of the most rational tori are visible as resonance chains (series of “ellipses”). The middle section illustrates mixed phase space dynamics with only one significant remaining region of regular motion. The right section illustrates chaotic dynamics. For values of $K \gg 5.0$, all the surfaces of section have the same global appearance. One can find very tiny regions of regular motion embedded in the chaos with good search methods, but they represent a microscopic proportion of the total phase space volume.

where $m, m' = 0, \dots, M-1$ are integers labeling the allowed discrete positions and the parameter K is the same kicking strength as for the classical rotor. Propagation of any initial state follows by repeated multiplication by \hat{U} to the time desired. If the initial state is expressed in a position basis, it is given as a column vector and Eq. (13) gives the form of \hat{U} ’s matrix elements to be used in the multiplication.

The single time step propagator is denoted as \hat{U} because it is a unitary matrix and therefore it has M eigenvalues $\exp(i\epsilon_k)$, $k = 1, \dots, M$, all of which lie on the unit circle. The (real valued) phases ϵ_k play a role very similar to the eigenenergies of quantum Hamiltonians, as mentioned for the Hydrogen atom. Similarly, for each eigenvalue $e^{i\epsilon_k}$ there is an associated eigenfunction or stationary state $\Psi_k(x)$ which is the analogue of the eigenstates of conservative quantum Hamiltonians.

One way to obtain a representation in phase space of the eigenfunctions $\Psi_k(x)$ is to construct the corresponding Husimi function $[\Psi_k]_H(x, p)$, which to each phase space point $\{(x, p)\}$ associates the value of the overlap between Ψ_k and a wave packet centered at position x and with mean momentum [velocity] p . Figure 3 shows such Husimi functions for various values of the kicking strength K . The structures of the classical phase space, such as displayed in Fig. 2, are somehow encoded in the quantum eigenstates. In the integrable limit or at very weak chaos the eigenstate Husimi functions are concentrated on invariant structures of the classical system. In the opposite limit of hard chaos, eigenstate Husimi functions are democratically, yet in some statistical way, distributed in the whole phase space, reminiscent of the ergodic exploration of phase space of chaotic trajectories. In the intermediate regime of mixed dynamics, for which classically chaos and regularity coexist, more complicated quantum structures emerge.

Concentrating for a moment on the very strongly chaotic systems, it turns out that the precise value of a particular eigenvalue or shape of a particular eigenfunction for given values of K, M carry little discernible information. The quantum system acts much like a pseudo-

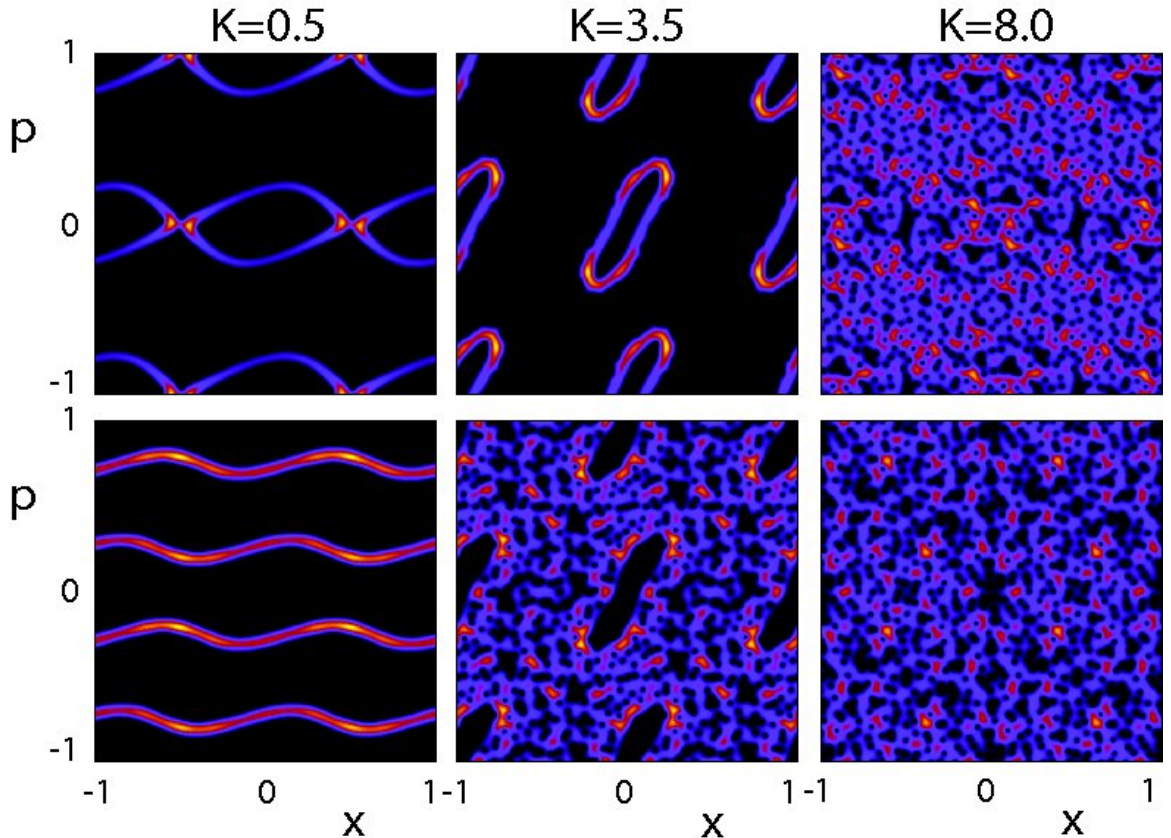


Figure 3: Husimi functions of eigenstates of the quantum kicked rotor. Two Husimi functions for each indicated value of coupling constant are shown in a vertical column. These figures are to be compared to the structures seen in Fig. 2. For $K = 0.5$, the classical dynamics are near integrable and almost entirely restricted to slightly distorted versions of the unperturbed tori or resonant tori. The lower eigenstate Husimi function can be seen to have the structure of such a distorted torus whereas the upper one corresponds to the separatrix of the largest resonance. For $K = 3.5$, the upper eigenstate Husimi function has the structure of a torus near the outer boundary of the regular region, and the lower one has its intensity in the chaotic region, which excludes the regular region. For $K = 8.0$, the Husimi functions cover the full phase space, albeit with fluctuations. For any very large- K system, these two Husimi functions are structurally characteristic of all of them. Husimi figures courtesy of Dr. Harinder Pal.

random number or state generator. Why this is so follows from considerations discussed ahead in Sect. 4. It is natural therefore to focus on the statistical properties of the eigenvalues and eigenfunctions. The result remarkably enough is related to the subject of random matrix theory, which is introduced in Sect. 5.

3.3 Classical emergence

The comparison between the classical phase space structure of Fig. 2 and the Husimi representation of quantum wave functions displayed on Fig. 3 illustrates for the kicked rotor system the deep connection that exists between classical and quantum dynamics. In particular, this quantum system has a qualitatively different behavior depending on whether the corresponding classical dynamics is in the regular or chaotic regime.

In the kicked rotor quantization, M plays the role of the inverse of Planck's constant. The larger M , the smaller $2\pi\hbar$. The classical dynamics must emerge from the quantum map as $\hbar \rightarrow 0$, but there is no single all encompassing perspective on how to envision this. One perspective is to create initial wave packets with minimum allowed uncertainty with respect to both position and momentum. For large M (small \hbar), it can be shown that for a short time scale known as the Ehrenfest time the center positions and momenta of nearly all wave packets follow the classical trajectory with the same initial conditions. Furthermore in the limit $M \rightarrow \infty$ ($\hbar \rightarrow 0$), it does so more and more exactly and for a growing Ehrenfest time scale, which approaches an infinite time logarithmically slowly if the system is chaotic.

This is essential for the Correspondence Principle, but it cannot be the complete story. For a fixed value of \hbar , there is a time after which the quantum dynamics no longer resembles the classical dynamics in the manner just described; a shorthand way of saying this is that the $\hbar \rightarrow 0$ and $t \rightarrow \infty$ limits do not commute. In addition, the information about the quantum dynamics after the Ehrenfest time up to a very long time scale known as the Heisenberg time (deriving from a time-energy minimum uncertainty principle), which is by far the greater time scale, is encoded in the eigenvalues and eigenfunctions that are the key quantum properties in which one is often most interested. It would seem as though the eigenproperties have little to do with any relation to the classical dynamics in the $\hbar \rightarrow 0$ limit. As we have just seen above, this turns out not to be true and the quantum-classical correspondence beyond the Ehrenfest time scale is much deeper than initially believed possible. Beyond the simple qualitative observation that we could make by inspection of the kicked rotor Husimi functions, it has more generally a number of consequences for the eigenproperties, statistically speaking and otherwise. This implies in particular that information about the classical chaos structures, including the rather complex homoclinic and heteroclinic tangles uncovered by Poincaré, must somehow be mysteriously embedded in the eigenproperties as well.

4 Semiclassical description of chaotic systems

With the kicked rotor and more generally, a deep connection exists between the behavior of a quantum system and the more or less chaotic nature of its classical analog. This connection clearly stems from the fact that classical dynamics can be seen as the limit as \hbar goes to zero of the more fundamental theory which is quantum mechanics. Even without entering into the discussion of decoherence phenomena, this limit is nontrivial and requires some degree of formalism to be described properly. This section contains a brief overview of some of the tools that can be used in a semiclassical regime (small \hbar). We consider first the Bohr-Sommerfeld quantization rule mentioned in the introduction, which actually applies only to integrable systems, before continuing with the description of more modern tools that can be used for other dynamical regimes.

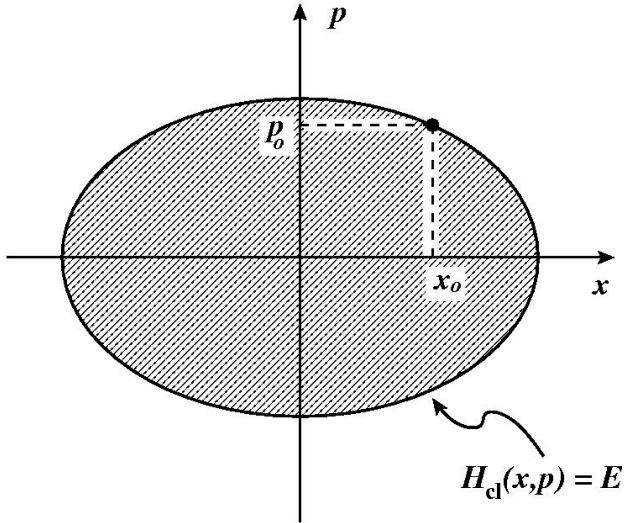


Figure 4: Sketch of a phase space trajectory initiated at some initial point (p_0, x_0) of energy $H_{\text{cl}}(p_0, x_0) = E$. The system is one dimensional, thus integrable, and therefore the trajectories identifies with the energy contour $H_{\text{cl}}(p, x) = E$. The shaded area corresponds to the action $J(E) = \oint p dx$ computed on this contour.

4.1 Bohr-Sommerfeld quantization rule

Let a time independent one degree of freedom system be described quantum mechanically by the Hamiltonian operator $\hat{H}_{\text{qu}} \stackrel{\text{def}}{=} -(h^2/2m)d^2/dx^2 + V(x)$, whose classical analog is $H_{\text{cl}}(x, p) = p^2/2m + V(x)$. Because H does not depend explicitly on time, the total energy is a constant of the motion, and thus, as sketched in Fig. 4, the phase space trajectories are confined on the 1-d curves $H(x, p) = E$, with E the initial energy. The integral

$$J(E) = \oint p dx \quad (14)$$

taken along this curve corresponds to the shaded area of Fig. 4, and has the dimension of an action, i.e. the same as the Planck constant $2\pi\hbar$.

The semiclassical regime can therefore be properly defined by the condition $J(E) \gg \hbar$. In this limit, it can be shown using a development of the Schrödinger equation in the small parameter \hbar that within a good approximation, the eigenenergies E_n of \hat{H}_{qu} are given by the condition

$$J(E_n) = 2\pi\hbar(n + 1/2) \quad n = 0, 1, 2, \dots, \quad (15)$$

(thus, what is quantized is the area enclosed by the energy contour). The semiclassical regime corresponds to large values of the quantum number n . Very precise approximations of the eigenfunction $\psi_n(x)$ can also be obtained within the same approximation scheme.

Up to the $1/2$ term [associated with the turning points of the classical trajectory], Eq. (15) is exactly the Bohr-Sommerfeld quantization rule of the Old Quantum Theory. It appears here however as an approximation derived within a controlled approximation scheme. For systems with d (larger than one) degrees-of-freedom, a generalization of this approximation scheme can be obtained *provided the system is integrable*. In that case, the classical trajectories in phase space are confined on d -dimensional manifold with the topology of a torus. The main difference is that an action integral can be defined for each of the generating paths of this torus, leading to d quantization conditions similar to Eq. (15), associated with d quantum numbers n_1, n_2, \dots, n_d . This generalization to $d > 1$ of the Bohr-Sommerfeld quantization rule, valid for integrable systems, is known as the Einstein-Brillouin-Keller (EBK) quantization rule.

4.2 Gutzwiller trace formula

The Bohr-Sommerfeld quantization rule and its generalization to systems with more than one degree of freedom provide a rather complete description of the eigenlevels E_n and eigenfunctions $\varphi_n(\mathbf{r})$ of quantum systems whose classical analogs are integrable. This semiclassical approximation scheme however strongly relies on the classical phase space being filled by invariant tori, which is a characteristic of integrable systems. Thus, it cannot be adapted to other kinds of dynamics. A completely different approach is required.

Semiclassical trace formulae provide such an alternative for the quantum spectral properties. They can be derived for a large range of dynamical regimes, including integrable, nearly integrable, fully chaotic, and (some) mixed phase space systems. Consider the fully chaotic regime, which leads to the Gutzwiller trace formula. The spectrum of \hat{H}_{qu} , i.e. the set of all energies E_1, E_2, \dots can be expressed in terms of the density of states function

$$d(E) \stackrel{\text{def}}{=} \sum_n \delta(E - E_n) , \quad (16)$$

with $\delta(x)$ the Dirac delta function. Quantum mechanically, $d(E)$ can be expressed in terms of the *trace* of the Green function $G(E) \stackrel{\text{def}}{=} [E - \hat{H}_{\text{qu}}]^{-1}$, hence the name of the approximation.

The density of states can, in most circumstances, be written as a sum of two contributions $d(E) = d_W(E) + d^{\text{osc}}(E)$, with $d_W(E)$ a smooth secular part associated with the classical system's energy surface phase space volume and which therefore can vary only on the classical scale. The remaining oscillating term, $d^{\text{osc}}(E)$, describes the short range, quantum fluctuations of $d(E)$.

A semiclassical trace formula links the purely quantum object, $d^{\text{osc}}(E)$, to a classical one, which turns out to be a sum running over all *periodic orbits* j of the classical motion. For chaotic classical dynamics the Gutzwiller trace formula is

$$d^{\text{osc}}(E) \equiv \frac{1}{\pi\hbar} \sum_j \frac{1}{\sqrt{\det(M_j - 1)}} \cos(\hbar^{-1}S_j - \nu_j\pi/2) , \quad (17)$$

where S_j , M_j and ν_j are classical quantities associated with the periodic orbit j at energy E . More specifically $S_j = \oint_{\text{orbit } j} \mathbf{p} d\mathbf{r}$ is the action integral along the orbit j , M_j is the monodromy matrix describing the stability of the linear motion near the orbit (the more unstable the orbit, the larger $\det(M_j - 1)$), and the Maslov index ν_j is an integer related to local winding around the orbit.

The Gutzwiller trace formula Eq. (17) is valid in the semiclassical regime, and expresses the strong link existing (in this regime) between a quantum system and its classical analog, even for chaotic dynamics for which the Bohr-Sommerfeld-style quantization rule does not apply. The mere existence of this connection leads to the expectation that the nature of the classical dynamics, and in particular its more or less chaotic character, must show up in the purely quantum properties of the system. In Sect. 5, the matter of how this takes place for statistical quantities related to the quantal spectrum or the eigenfunctions is addressed. First, it is worth making a few comments on the properties of the Gutzwiller trace formula and on the various ways it can be used in practice.

4.3 Orbit proliferation and convergence issues

The right hand side of the Gutzwiller trace formula Eq. (17), which expresses the classical sum over periodic trajectories, is divergent (how else could it create δ -functions), and thus requires some care to be properly defined. This property can be related to the exponential proliferation of periodic orbits in chaotic systems. Indeed, the degree of instability of a chaotic system

can be characterized by its Lyapunov exponent λ which measures the rate of divergence of generic neighboring trajectories. On the one hand, assuming periodic orbits behave as generic trajectories (which is mostly if not perfectly true), the monodromy matrix of a trajectory j is such that $\det(M_j - 1) \sim \exp(\lambda\tau_j)$, with τ_j the period of the orbit j . On the other hand λ also controls the total number of orbits of period τ_j smaller than some value τ , which grows as $\tau^{-1} \exp(\lambda\tau)$. The exponential smallness of $1/\sqrt{\det(M_j - 1)}$ cannot therefore compensate for the exponential proliferation of orbits. A more careful analysis here applicable to multi-degree-of-freedom systems leads one rather to the Kolmogorov-Sinai entropy, but the basic point of an exponentially increasing number of terms decaying as the square root in magnitude remains.

One simple way to cure this lack of convergence of the classical sum is to perform a local smoothing of the quantum density of states, or in other words to replace the Dirac peaks $\delta(E - E_n)$ in Eq. (16) by a function $\delta_\epsilon(E - E_n)$ with a finite width ϵ (but still of integral unity). This can be done simply for instance by giving a small imaginary part ϵ to the energy (i.e. $E \rightarrow E + i\epsilon$), which amounts to use a Lorenzian function $\delta_\epsilon(E - E_n) = \pi^{-1}\epsilon/[(E - E_n)^2 + \epsilon^2]$. In that case, each term in the periodic orbit sum of Eq. (17) is multiplied by an exponentially small term $\exp[-\epsilon\tau_j/\hbar]$, in such a way that all orbits of period $\tau_j > \tau^*(\epsilon) = \hbar/\epsilon$ are effectively cut off from the sum.

There can be very different motivations for local smoothing of a quantum spectrum. For a first example, one may not be interested in the details of the spectrum, either by choice, or because these details simply cannot be accessed experimentally. This can arise if the interaction with the surrounding environment gives a finite coherence time, that broaden the energy levels, to the system. Another natural source of smoothing is simply the existence of a finite temperature, which when describing the thermodynamic properties of some system can be seen as causing a local averaging on an energy scale $k_B T$ (and thus trajectories of period $\tau_j \gg \hbar/(k_B T)$ do not contribute to the thermodynamic properties of the system under consideration). In some circumstances, the scale at which one wants to probe the quantum spectrum is rather large, and can be in particular much larger than the mean level spacing Δ [i.e. the average energy spacing between two successive energy levels]. When probing the thermodynamic properties of micron-sized quantum dots in a GaAs/AlGaAs hetero-structure, the mean level spacing is roughly $\simeq 3 \times 10^{-4}$ meV. However, a dilution refrigerator is typically limited to temperatures of the order of a 100mK, which corresponds to roughly 9×10^{-3} meV. In that case, only rather short orbits (sometimes just a few) survive the averaging and the Gutzwiller trace formula (or its analogue in other dynamical regimes) provides both a precise prediction and an intuitive interpretation of the quantum physics under consideration in terms of a few sets of classical periodic orbits. Examples where such approaches have been extremely fruitful includes the above mentioned thermodynamic properties of ballistic quantum dots as well as stability properties of small metallic wires.

4.4 Breaking the mean level spacing scale

More delicate is the situation where one wants to describe semiclassically the fine structure of the spectrum. To resolve the mean level spacing, Δ , which for a system with d degrees of freedom scales as \hbar^d , very long orbits – with a period τ_j larger than the Heisenberg time $t_H = \hbar/\Delta \sim \hbar^{d-1} \xrightarrow{\hbar \rightarrow 0} \infty$ – need to be included in the semiclassical sum. The number of such orbits grows extremely rapidly. (In the hyperbola billiards for instance, there are only 1061 orbits with less than $N = 9$ bounces off the boundary of the billiard, but already 136 699 for $N = 14$.) Even if the semiclassical sum can be made formally convergent by choosing a smoothing ϵ finite but much smaller than Δ , two difficulties need to be addressed.

The first one is simply to decide if the semiclassical approximation is still valid for such long orbits. Indeed, it is known that the limits $\hbar \rightarrow 0$ and $t \rightarrow \infty$ do not commute, or in

other words, that for any finite \hbar , there is a critical time scale t^* beyond which semiclassical approximations should not be correct any more. A natural question then is whether t^* is larger than the Heisenberg time t_H , in which case there is a hope that individual energy level can be resolved within the trace formula framework.

It was first suggested that t^* could be identified with the Ehrenfest time t_E , namely the time associated with the spreading of a wave-packet in the entire available phase space. Because of the exponential divergence of trajectories, t_E has a logarithm dependence in \hbar and is therefore a time scale significantly shorter than the Heisenberg time necessary to resolve the mean level spacing. Work on three paradigms of chaos, the baker map, the Bunimovich stadium billiard, and kicked rotor however showed that it was in fact possible to propagate wave packets semiclassically for time significantly longer than the Ehrenfest time t_E , and thus that this is not particularly a limitation of the time for which semiclassical approximations can be used. Investigations on these systems furthermore gave a theoretical foundation to this “long term accuracy”. These studies however pointed out that, for these systems, diffraction effects should prevent reaching the Heisenberg time in the deep semiclassical limit, although in practice the approximation usually seems to work better than expected, and the Heisenberg time could be reached for the (already significant) energies investigated.

Even if one is interested in a configuration such that t^* is larger than t_H – either by not going too deep in the semiclassical regime, by treating semiclassically the diffraction terms, or by considering systems for which the semiclassical trace formula is actually exact – another issue related to the proliferation of orbits has to be considered. The mathematical statement that the semiclassical sum in the Gutzwiller formula is divergent has a practical consequence that for the contribution of long orbits to remain finite, a great amount of cancellation has to take place between the various terms in the semiclassical sum. To derive individual energy levels from the semiclassical expansion in term of periodic orbits it is therefore necessary to understand how these cancellations take place, and what is the structure in the organization of the classical periodic orbits that allows these cancellations to occur.

Important progress in this respect has come simply by introducing mathematical objects with less singular behavior than the density of states when considered at the sub-mean level spacing scale. Indeed, even if one assumes a smoothing on a scale ϵ ($\ll \Delta$) has been performed to regularize the semiclassical sum, the presence of the Dirac delta functions in Eq. (16) implies that the density of states has to switch from zero to $1/\epsilon$ on a distance of order ϵ . This enhances the high frequency contributions, and thus the role of long period orbits. Quantities such as spectral determinants which, up to some proper regularization, can be defined as

$$\mathcal{D}(E) \equiv \prod_n (E - E_n) \tag{18}$$

just go to zero each time E reaches an eigenenergy of the system, and are therefore less singular. Semiclassical expansions in terms of periodic orbits can be written for these spectral determinants, sometimes in conjunction with the use of functional equations, and the corresponding semiclassical sums show less divergence. Other ways to express the quantum spectrum, for instance through the use of dynamical zeta functions have also been introduced for similar reasons.

Beyond these rather formal issues, a better understanding of the structure of long periodic orbits has helped control the semiclassical periodic orbit expansions. Consider for instance the three disc system illustrated in Fig 5. Also shown on this figure are a couple of short orbits, corresponding respectively to 2 and 3 bounces, and a longer one. Within a good approximation, longer orbit can be decomposed into a succession of shorter ones pieced together. Taking advantage of this approximate decomposition, Cvitanovic and co-workers have introduced a “cycle expansion”, which, by regrouping terms appropriately, increases significantly the convergence properties of the semiclassical expansion.

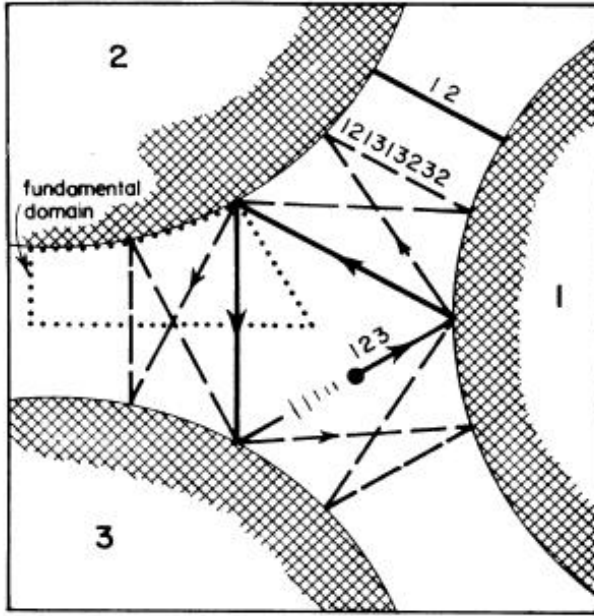


Figure 5: The three disc billiard, together with three periodic orbits of this system. A code, formed from the label of the disc hit successively, is associated to each orbit. Reprinted figure with permission from [P. Cvitanović and B. Eckhardt Phys. Rev. Lett. **63** pp 823–826 (1989)]. Copyright (1989) by the American Physical Society.

Semiclassical trace formulae therefore provide a link between a quantum system and its classical analogue through the expression of the (quantum) energy spectra in terms of the (classical) periodic orbits. If only a coarse grained approximation of the spectra is required, only short orbits are involved, providing in this way a simple and transparent interpretation of the quantum behavior. Accessing the finer details of the quantum spectra, and in particular resolving the mean level spacing, implies considering much longer orbits. This requires the use of more sophisticated techniques, in particular the introduction of mathematical tools such as spectral determinants or dynamical zeta functions coupled with cycle expansions.

5 Random Matrix Theory

As mentioned in the previous section, the mere existence of semiclassical approximations such as the Gutzwiller trace formula, which creates a link between a quantum system and its classical analog, implies that the qualitative nature of the classical dynamics should show up in some ways in the quantum mechanical properties. Of course, this was already implied for the eigenstate structure by the Einstein-Brillouin-Keller quantization, and its inability to predict eigenstates for chaotic systems as was clearly illustrated by the Husimi functions in Fig. 3. However, the trace formula implies that statistical properties of spectra depend on the difference between classically integrable/regular systems and chaotic ones, and that it is possible to be quantitative. Consider the spectra of the kicked rotor in Fig. 6. The spectrum of the near-integrable case on the left intrinsically exhibits a much greater number of large gaps or close-lying levels than the strongly chaotic case on the right. Understanding these properties quantitatively is the goal of the subject of spectral statistics.

One of the most important tools is random matrix theory, which was introduced for the spectral statistics of strongly interacting many-body systems well before the dynamical distinctions and their effects were understood, and before the Gutzwiller trace formula existed. Since

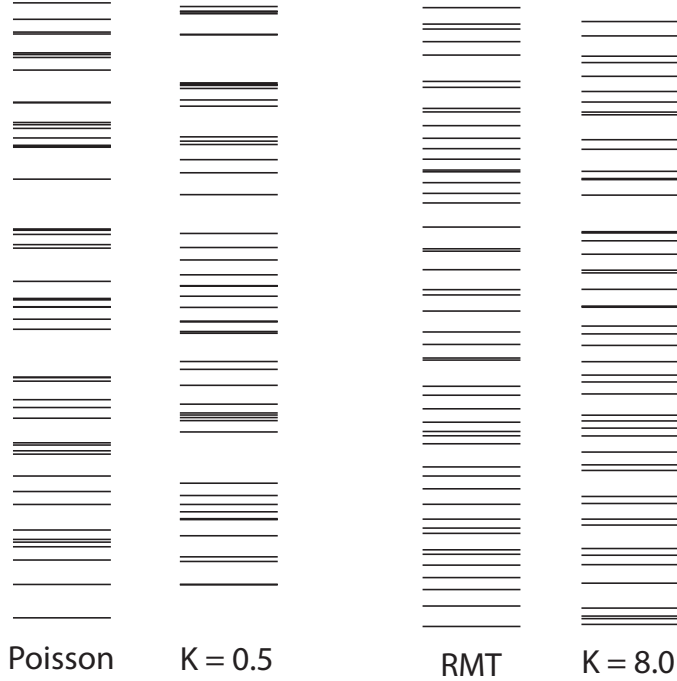


Figure 6: Two spectra of the kicked rotor compared with two statistical limits. Fifty levels of the $K = 0.5$ spectrum are plotted with the vertical axis indicating increasing eigenangle. It is in the near-integrable regime and can be seen to be qualitatively very much like the Poisson spectrum, which results from a complete absence of correlations. On the other hand, the $K = 8.0$ spectrum is qualitatively like the so-called random matrix spectrum.

then the role of chaos and the link between trace formulae and random matrix theories has come to light. It is worth noting a beautiful and highly nontrivial example of the deep connections between such seemingly disparate concepts as chaotic trajectories and random matrices that has come to light in studying spectral statistics. As briefly mentioned in the introduction, random matrix theory implies universality in statistical properties, i.e. the notion that much of the system specific information vanishes from statistical properties such as the spectral statistics. One might be tempted to think that although each chaotic system may have chaotic trajectories, the trajectories themselves are still system specific, and so the system information still matters. However, it turns out that for all chaotic systems the necessary set of chaotic trajectories for the description of their quantum counterparts, weighted by their instabilities, uniformly explore their respective phase spaces, and it is this uniformity that implies a loss of information precisely equivalent to that implied by universality in random matrix theory.

5.1 Spectral statistics

Consider a quantum Hamiltonian \hat{H}_{qu} and H_{cl} its classical analog. Near some arbitrary energy \bar{E} that is large in comparison to the ground state energy, it is useful to introduce three energy scales. The first one δE_{cl} is the scale at which the classical dynamics changes appreciably. δE_{cl} is a purely classical quantity and has therefore no \hbar -dependence: $\delta E_{\text{cl}} \sim \hbar^0$. The two other energy scales are quantum ones: the mean level spacing Δ already introduced, which behaves as $\sim \hbar^d$ (with d the number of degrees of freedom), and the Thouless energy $E_{\text{Th}} = \hbar/t_{\text{fl}} \sim \hbar$, where the “time of flight” t_{fl} is the typical (classical) time necessary to cross the system (at energy \bar{E}).

In the semiclassical limit $\hbar \rightarrow 0$, and assuming two degrees of freedom or more, there is

a separation between these different energy scales: an energy range which is small compared with δE_{cl} , and within which the classical dynamics remains essentially constant, may contain an infinite number of slices of energies E_{Th} , each of them containing an infinite number of energy levels. A relatively simple semiclassical reasoning – based actually on the Gutzwiller trace formula discussed in Sect. 4 – shows that energy levels separated in energy by a distance larger than the Thouless energy are essentially independent of each other. Each energy slice E_{Th} can therefore be considered as an independent realization of some statistical ensemble and for any spectral quantity $f(\{E_i\})$ the statistical expectation $\langle f \rangle$ can be defined as the corresponding mean on the various energy slices, which in practice implies that a local energy average is performed in an energy range δE which is negligibly small on the scale δE_{cl} but is large on the scale E_{Th} .

The simplest quantity that can be defined in this way is the mean density of states $\langle d(E) \rangle \stackrel{\text{def}}{=} \langle \sum_n \delta(E - E_n) \rangle$ which counts the average number of energy levels in an energy interval of length one. The mean level spacing Δ is the inverse of $\langle d(E) \rangle$. The average density of states $\langle d(E) \rangle$ is however essentially determined by the volume of the classical energy surface $H_{\text{cl}}(\mathbf{r}, \mathbf{p}) = E$, and is thus independent of the more or less chaotic nature of the classical motion. To focus on the energy level correlations, which turn out to depend on the nature of the classical dynamics, it is helpful to perform a [locally linear] scaling to transform the original eigenenergies $\{E_1, E_2, E_3, \dots\}$ into a rescaled sequence $\{x_1, x_2, x_3, \dots\}$ with the same fluctuations properties, but a mean density one [locally, one can think of the transformation $\{E_i\} \rightarrow \{x_i\}$ as a multiplication by $\langle d(E) \rangle$].

A few interesting quantities can be constructed to measure the fluctuation properties of the $\{x_i\}$. Consider for instance $N_E(r)$ which counts the number of rescaled levels x_i in an interval of length r near the energy E . By construction $\langle N_E(r) \rangle = r$ since the average density of x_i 's is one, however

$$\Sigma^2(r) = \langle N_E^2(r) \rangle - \langle N_E(r) \rangle^2 \quad (19)$$

which measures the variance of $N_E(r)$, contains useful information about the fluctuation properties of the spectrum. For example, for small r it tells us about the likelihood of levels to cluster at short ranges, and for large r , it tells us how elastic or rigid the spectrum is. Another important quantity is the nearest neighbor density $P(s)$, which measures the probability that two successive [rescaled] levels x_i and x_{i+1} are separated by a distance s . $P(s)$ probes only the short range fluctuation properties of the spectrum. Many other statistical quantities have been introduced and can be found in the literature. One can cite the two point correlation function $R_2(s)$, the Dyson cluster function $Y_2(s)$, or the $\Delta_3(r)$ function which measures the deviation of $N_E(r)$ from the best straight line. Here, it is enough to consider $P(s)$ and $\Sigma^2(r)$.

For these two statistics, it is worthwhile to calculate their values for the simple case of a *Poisson* sequence of energies, i.e. the $\{x_i\}$ are independent numbers taken at random with a mean density one. In this case,

$$P_{\text{Poisson}}(s) = \exp(-s) \quad (20)$$

$$\Sigma_{\text{Poisson}}^2(r) = r. \quad (21)$$

Poisson statistics correspond to the limiting case of a total absence of correlation. For a given spectrum, how far the resulting statistical quantities differ from the Poissonian case thus provides a first quantitative glimpse into the presence of correlations.

5.2 Random Matrix Ensembles

Random matrix ensembles were introduced into physics by Wigner in the fifties in the context of nuclear physics. His goal at that time was to describe the statistical properties of slow neutron resonances, which correspond to highly excited states of a nuclei. Because of this high

energy, and because nuclei, except for the smaller ones, can be considered as “complex” systems, in the sense that they have a very large number of degrees of freedom [already about 150 for iron] interacting strongly through complicated interactions, Wigner came to the conclusion that individual evaluation of these energy levels was presumably an unachievable task, and not necessarily a very useful one either. On the other hand, the very complexity of the nuclei Hamiltonian makes it reasonable to describe its statistical properties in terms of random matrices.

Indeed, a quantum Hamiltonian, whether it describes a nuclei or, as in Eq. (7) the much simpler Hydrogen atom, is a linear “operator” acting on the space of wavefunctions, which means that it can be represented as a matrix. As the vector space of wavefunctions has an infinite dimension, this matrix is also infinite, but it is natural to model the neighborhood of some energy \bar{E} with a finite (but large) $N \times N$ matrix. The idea of Wigner was that because of the complexity of nuclear dynamics, their spectral statistics – experimentally accessible through the neutron resonances – should be the same as for matrices whose matrix elements are taken *as random as possible*.

There are however some limitations to this randomness as some constraints on the matrix (H_{ij}) representing the quantum Hamiltonian should be implemented. First of all, the Hamiltonian governs the time evolution of quantum wavefunctions, and this evolution has to be *unitary* (the square modulus of the wave function is a probability, so its sum over all possible configurations has to be one). This implies in particular that the Hamiltonian matrix has to be, at the very least, Hermitian: for any pair (i, j) , the entry H_{ij} should be the complex conjugate of H_{ji} . Therefore, once the lower diagonal of the matrix is fixed, in fact all matrix elements are determined.

Beyond this basic constraint due to the unitarity of the quantum evolution, other constraints, associated with the symmetry of the problem under consideration, have to be taken into account. For instance, the Hamiltonians describing nuclei are invariant under a rotation of the physical space, which implies that the vector subspace corresponding to different kinetic momentum quantum numbers should be considered independently. More generally, whenever a symmetry implies the existence of good quantum numbers, the statistical analysis has to be performed for a fixed value of these quantum numbers.

One symmetry plays a particularly important role, namely the invariance with respect to time reversal. For a classical system, the motion is said to be time reversal invariant if for any phase space trajectory $(\mathbf{r}(t), \mathbf{p}(t))$, the trajectory $(\mathbf{r}(-t), -\mathbf{p}(-t))$ is also a solution of the equations of motion. Similarly a quantum Hamiltonian is time-reversal invariant if for any solution $\Psi(t)$ of the time dependent Schrödinger equation Eq. (6), $\Psi^*(-t)$ is a solution too. Time reversal symmetry can be broken by the application of an external magnetic field. Limiting our discussion to system without spin, it can be shown that one can construct a basis for which *all time reversal symmetric Hamiltonians* have real (rather than complex) matrix elements. Together with the requirement that the time evolution is unitary, this implies that time reversal invariant Hamiltonians can be taken as real symmetric matrices.

To implement the notion of maximum randomness within these constraints, Wigner has introduced three random matrix ensembles. The first one is the Gaussian Unitary Ensemble (GUE), which corresponds to systems for which time reversal invariance is broken. In that case the entries $H_{i,j}$ of the matrices are complex numbers taken (for $i > j$) as independent random variables following a Gaussian distribution with an arbitrary, but fixed, width. The upper diagonal part $i < j$ then follows from the hermiticity of the matrix, which also imposes a slightly different treatment for the diagonal elements. If time reversal symmetry is preserved, and in the absence of spin degrees of freedom, the corresponding ensemble is the Gaussian Orthogonal Ensemble (GOE) which is constructed in a similar way as GUE except that the entries H_{ij} are real, rather than complex, numbers. Finally a third ensemble, the Gaussian

Symplectic Ensemble (GSE) has been introduced by Wigner to model time reversal invariant system with spin degrees of freedom, and constructed on the basis of quaternions. Here only the GOE and GUE cases are discussed.

The value of spectral statistics, such as $P(s)$ or $\Sigma^2(r)$ have been computed for these ensemble. For the nearest neighbor distribution $P(s)$, good approximations are provided by the “Wigner surmise”

$$P_{\text{GOE}}(s) = \frac{\pi}{2} s e^{-\pi s^2/4}, \quad (\text{GOE}) \quad (22)$$

$$P_{\text{GUE}}(s) = \frac{32}{\pi^2} s^2 e^{-4s^2/\pi} \quad (\text{GUE}). \quad (23)$$

Compared with the corresponding Poisson statistics Eq. (20), these distributions are characterized by a rather strong *level repulsion*. Indeed, whereas for an uncorrelated spectrum the most probable spacing is actually zero (if nothing prevents it, the nearest neighbors can be very close to each other), for the random matrix ensembles there is a null probability to find zero-distance spacings, and for small spacings this probability grows only linearly in the GOE case and even more slowly in the GUE case.

Exact expressions exist also for the $\Sigma^2(r)$ statistics of the random matrix ensembles. The details of the expressions are too opaque for our purposes here, but the large r asymptotic in the GOE case reads

$$\Sigma_{\text{RMT}}^2(r) \simeq \frac{2}{\pi^2} \ln(r) \quad (r \gg 1), \quad (24)$$

and is half this value for the GUE. Compared to Eq. (21), the random matrix statistics show a strong *level rigidity*. Consider for instance an interval of length 100, which therefore contains on average one hundred rescaled levels x_i . In the Poissonian case, Eq. (21) expresses that for any particular realization one expects to find most often a number between 90 and 110 levels in a given interval. In the random matrix theory (RMT) case on the other hand, Eq. (24) tells us that the typical fluctuation around the mean value is $\sqrt{\frac{2}{\pi^2} \ln(100)} \simeq 0.97$ if time reversal invariance is preserved, and $1/\sqrt{2}$ times this value if it is broken. Even for such a long sequence, a typical realization will contain exactly one hundred level plus or minus maybe one level.

5.3 Quantum chaos and Random matrices

The random matrix ensembles such as GOE or GUE provide random realizations of model Hamiltonians for which spectral statistics such as the nearest neighbor distribution $P(s)$ or the $\Sigma^2(r)$ statistics can be evaluated and compared to the predictions of other models or to experimental data. In the case of nuclear resonances, the comparison showed a very good agreement between the RMT predictions and the nuclear spectral statistics.

As mentioned above Wigner, and others, were expecting this agreement on the basis of the complex character of the nuclear dynamics. In 1984 however, Bohigas, Giannoni and Schmit suggested that even “simple” systems could display the same kind of statistical behavior. Indeed, performing a numerical analysis of two-dimensional billiards such as Bunimovich’s stadium billiard, they showed that these systems displayed also random-matrix-like statistics. Illustration for the $P(s)$ statistics corresponding to the stadium billiard is shown on Fig. 7 together with the corresponding RMT and Poisson statistics. Dynamical systems such as the stadium billiard are definitively not complex systems: they have only two degrees of freedom and their Hamiltonian contains only a kinetic energy term. They are however chaotic.

This led Bohigas, Giannoni, and Schmit to conjecture that even “simple” systems would display the spectral fluctuations of the random matrix Gaussian ensembles *provided the dynamics of their classical analog was chaotic*. From this perspective, the role of complexity for nuclei

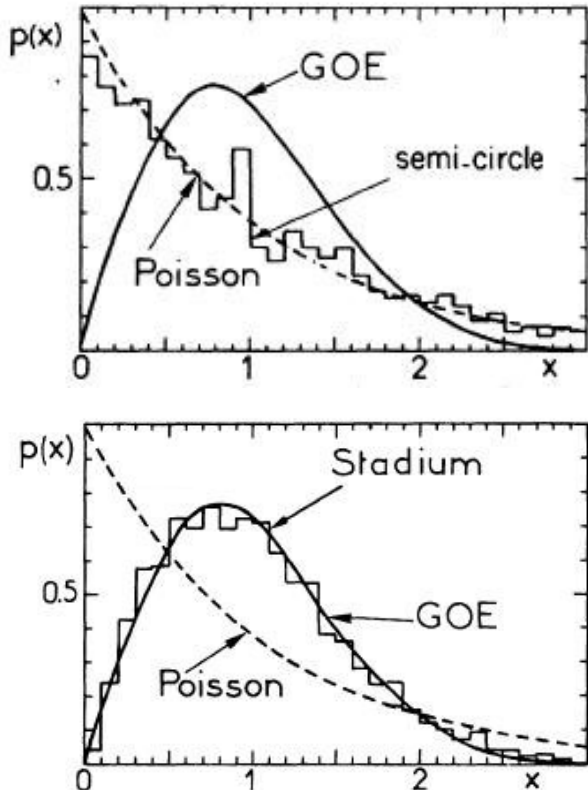


Figure 7: Nearest neighbor density: (bottom) for the Bunimovich stadium billiard (chaotic); (top) for the semicircular billiard (integrable). For chaotic dynamics, the distribution agrees perfectly well with the Wigner surmise Eq. (22) valid for the GOE ensemble (solid line). On the other hand, for the integrable case $P(s)$ perfectly matches the Poisson distribution expected for uncorrelated levels (dashed line). Reprinted with permission from [O. Bohigas, M. J. Giannoni, and C. Schmit, J. Physique Lett. **45** pp 1015-1022 (1984)] <http://dx.doi.org/10.1051/jphyslet:0198400450210101500>.

is just to provide a chaotic dynamics, and it therefore loses the central character it had in the spirit of Wigner. Although, there is not yet a complete formal proof of the Bohigas, Giannoni, and Schmit (BGS) conjecture, it is, beyond a large body of numerical evidence, strongly supported by semiclassical theory. Indeed, it was first shown by Berry that the logarithmic level rigidity predicted by random matrix for the number variance emerges from calculations based on the Gutzwiller trace formula. These calculations, which addressed the long range behavior of the spectral statistics, relied only on the uniformity principle of Hannay and Ozorio that states that periodic orbits of chaotic systems explore the phase space uniformly once weighted by their inverse stability determinants. Introducing a loop expansion very similar to the Hikami boxes of weakly diffusive systems, Sieber and Richter lead the way to a series of results extending this connection between semiclassical trace formulae and random matrices to a large set of spectral statistics and for all energy ranges. Remarkably, two mathematical objects seemingly disparate, a sum over periodic orbits and random matrix ensembles, are inextricably linked.

If chaotic systems display RMT-like fluctuations properties, it has been shown by Berry and Tabor that *integrable* systems display spectral statistics much closer to the Poissonian case, and in particular show neither level repulsion nor level rigidity. Spectral statistics therefore provide a clear signature of the nature of the classical dynamics in these two extreme cases. The intermediate situation of mixed dynamics, where chaos and regularity coexist in the classical phase space, has also been considered. The situation there is somewhat more complex, as the existence of some non-universal time scales has to be implemented, giving rise to transition matrix-ensembles lacking the universal character of the original and otherwise featureless Gaussian ones.

Returning to Fig. 6, applying the statistical theory above to the kicked rotor suggests that the near-integrable regime, as pictured on the left, should have statistics which are typically more like a Poisson spectrum than that of random matrix theory, whereas the strongly chaotic case pictured on the right should be the opposite. This is exactly what is seen with the comparison of a sample Poisson and random matrix spectrum shown there. The propensities for small spacings and long range rigidity in the spectra of the kicked rotor, depending on the dynamical regime, turn out to be in quantitative agreement with the Poisson and random matrix limits. Performing larger calculations to reduce statistical sample size errors and being careful with the dynamical limits leads to excellent agreement with the expressions given in the previous two subsections.

As a final remark, random matrix theory, or rather quantum chaos, has been linked to some very important mathematical relations. In particular, there is the connection to the Riemann zeta function and Riemann hypothesis that all non-trivial zeros of this function have real part one half and differ only in their imaginary parts. The values of these imaginary components can be thought of as a spectrum, and it turns out that their statistical properties match precisely those of the GUE. That spectrum furthermore has an analog of the Gutzwiller trace formula called the Selberg trace formula, which was discovered earlier and happens to be exact for the Riemann zeta function. Thus, the Riemann zeta function, in addition to its previous mathematical importance, has the developed the status of being a sort of mathematically rigorous playground for studies of quantum chaos.

6 Physical applications

Having introduced the main tools developed in the context of quantum chaos, and in particular the semiclassical approximations and the random matrix models, we shall finish this introductory review by a brief description of a few physical examples for which these tools have proven useful. Our goal here is neither to be exhaustive nor to be thorough, but rather to provide a few entry points to some interesting physical illustrations of the subject, and to the corresponding

literature.

6.1 The Hydrogen atom in a strong magnetic field

First consider the Hydrogen atom in a strong magnetic field. Immersing a Hydrogen atom within a strong magnetic field (in the range of a few Tesla) and measuring its spectra has been done in the laboratory since the mid-nineteen eighties. The Hydrogen atom is also simple enough (assuming the proton infinitely heavy, this is a “one particle problem”) that its spectra can be computed rather precisely through numerical approaches (which nevertheless may require some degree of sophistication).

Even in the presence of a magnetic field – assumed along the z direction – the Hydrogen atom remains invariant under a rotation around the z -axis and under reflexion of the z -axis. This implies the existence of two good quantum numbers: m , associated with the angular momentum projection J_z , and $\pi = (+, -)$ associated with the reflection symmetry. For the sake of illustration, let us consider the $m^\pi = 1^+$ subspace. Results of a numerical calculation for a part of the spectra within this subspace are displayed in Fig. 8. Inspection of this figure shows some regular patterns on the left – weak field – side of the figure. These patterns can be understood as arising from the perturbation of the original Hydrogen atom spectra by a weak magnetic field. In this regime, groupings of levels converge at zero field toward the same Hydrogen atom energies whose label n characterizes the corresponding state subspace. In the opposite regime of very high magnetic field (not shown on this figure), one would also recognize the Landau level structure that one would get with the magnetic field alone, only slightly perturbed by the electric field generated by the nuclei of the atom. Both regimes (weak and strong field) can be understood as a perturbation around a known limit, which allows both for a good qualitative understanding and for practical ways to perform calculations going beyond numerical approaches.

The intermediate field regime seems however a priori to contain significantly less obviously visible “features”. Energy levels appear to follow a seemingly erratic evolution as a function of the magnetic field with no clear emerging patterns. Observing the information contained in these data in the proper way shows however that this is actually not the case.

The quantum mechanics of the Hydrogen atom in a magnetic field varies both with the magnetic field B and with the energy E at which the dynamics is considered, both parameter being essentially independent variable. This is not the case however for the classical analog of this system. Indeed, it can be seen that the dynamics depend only on the scaled energy $\epsilon \stackrel{\text{def}}{=} E\gamma^{-2/3}$, where γ is a dimensionless parameter proportional to B (see caption of Fig. 8 for the precise definition), but not on the energy and the field independently. In other words, different fields and energies corresponding to the same ϵ leads to exactly the same classical trajectories (up to a rescaling of the dynamical variables).

Fig. 9 shows a few Poincaré sections describing the classical dynamics corresponding to $J_z \equiv 0$. These Poincaré sections represent the intersection of a trajectory in phase space with a given hyper-plane and the energy surface, and are the equivalent, for time-independent systems of the stroboscopic map used in Sect. 3 for the kicked rotor model (see Fig. 2). We see there that as ϵ varies from zero to $-\infty$, the dynamics goes from almost integrable (actually a perturbation of the Hydrogen atom without magnetic field) to chaotic. One expects as a consequence that the spectral statistics will reflect this evolution of the nature of the dynamics as ϵ varies. And indeed, this is what is observed in Fig. 10, where the nearest neighbor distributions corresponding to the two extreme dynamical regime are shown, and a transition between Poisson and GOE is observed. Other statistics, as well as the intermediate regime of mixed dynamics have been investigated, confirming on this particular example the links between the nature of the classical dynamics and spectral statistics.

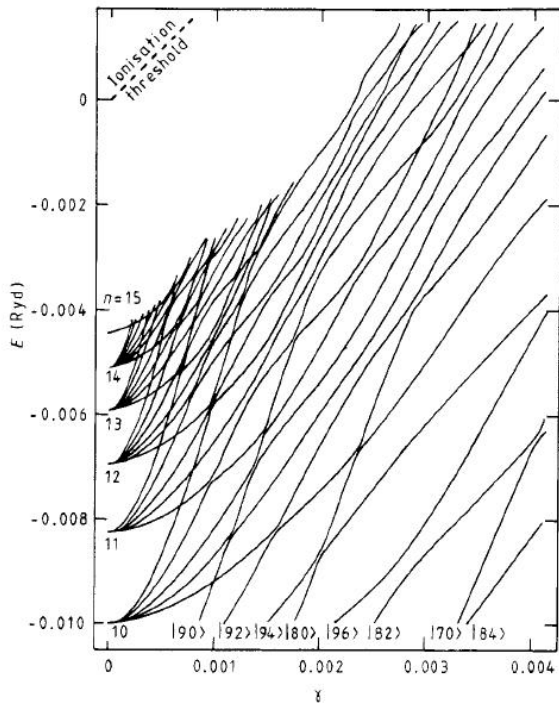


Figure 8: Part of the bound state spectrum in the $m^\pi = 1^+$ subspace showing states from the n -manifolds around $n \simeq 12$. γ is the ratio between the energy scale defined as \hbar times (half) the cyclotron frequency $\frac{1}{2}(eB/2m_e)$ and the Rydberg energy $\mathcal{R} = m_e e^4 / 2\hbar^2 \simeq 13.6$ ($\gamma = 2 \cdot 10^{-5} \simeq 4.7$ T). This figure is taken from [D. Wintgen and H. Friedrich, J. Phys. B: At. Mol. Phys. **19** (1986) pp 991-1011]. ©IOP Publishing. Reproduced with permission. All rights reserved.

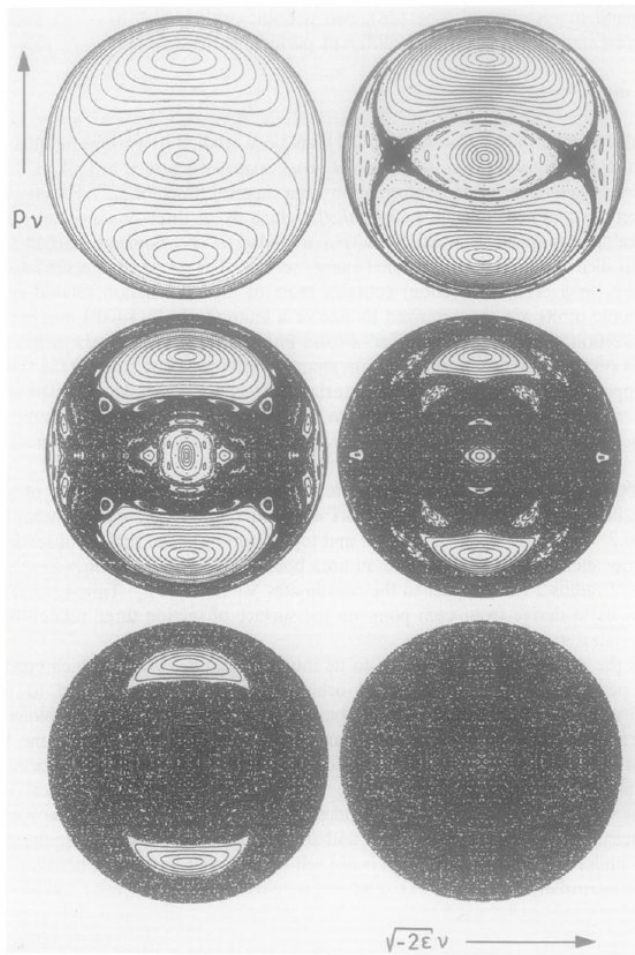


Figure 9: Poincaré surfaces of section (for $J_z = 0$ and using semi-parabolic coordinate) at $\epsilon = -0.8, -0.5, -0.4, -11.3, -11.2$ and -11.1 (from left to right and top to bottom). Reprinted from [Phys. Rep. **183**, H. Friedrich and D. Wintgen, pp 37–79 Copyright (1989)] with permission from Elsevier.

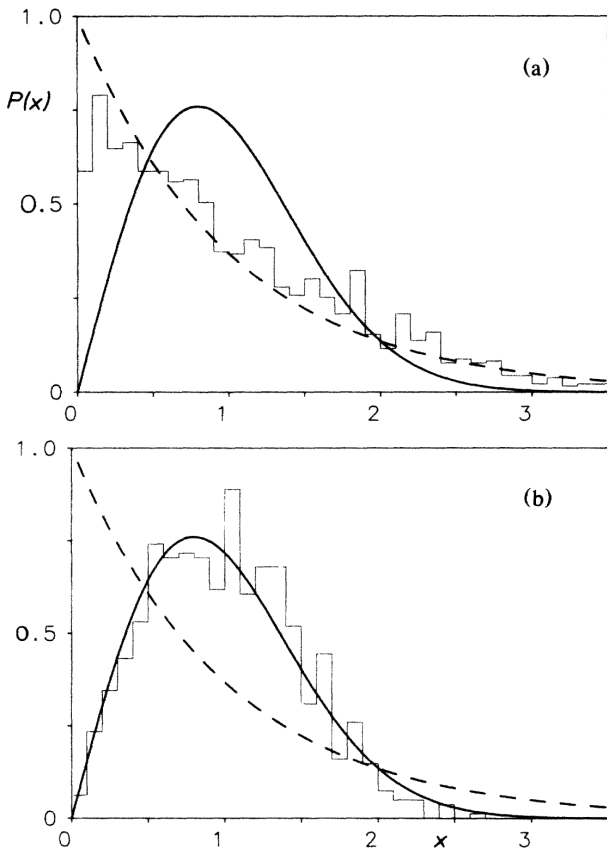


Figure 10: Nearest neighbor distribution for the Hydrogen atom in a magnetic field. Upper panel: regular regime (corresponding to the upper Poincaré sections of Fig. 9). Lower panel: chaotic regime (corresponding to the lower Poincaré sections of Fig. 9). The solid line and dashed line correspond respectively to the Gaussian Orthogonal Ensemble (GOE) predictions expected for chaotic systems and to the Poisson prediction associated with integrable dynamics. Reprinted figure with permission from [D. Wintgen and H. Friedrich, Phys. Rev. Lett. **57** pp 571–574 (1986)]. Copyright (1986) by the American Physical Society.

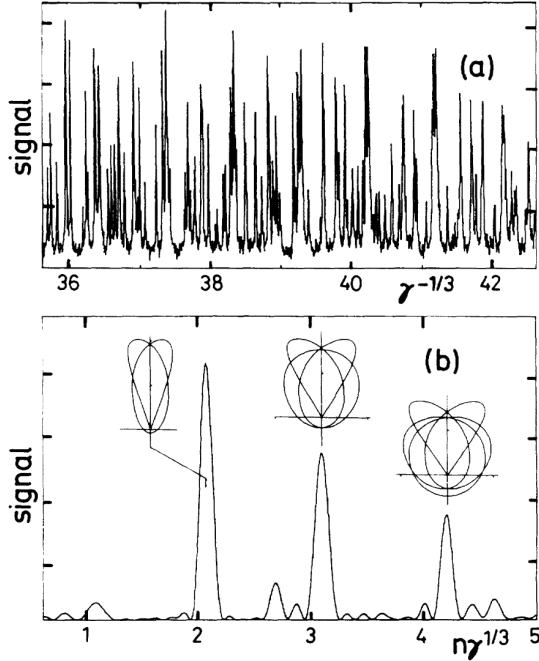


Figure 11: (a) Spectrum of the Hydrogen atom at a fixed value $\epsilon = -0.45$ of the scaled energy, as a function of $\gamma^{-1/3}$. (b) Fourier transform of (a) and corresponding periodic orbits. Reprinted figure with permission from [A. Holle *et al.*, Phys. Rev. Lett. **56** pp 2594–2597 (1986)]. Copyright (1986) by the American Physical Society.

In the same way that the spectral statistics encode the nature of the classical dynamics, the periodic orbits, and in particular their length (action) spectrum organize the quantum data. This is illustrated in Fig. 11 showing experimental data by Holle and coworkers of the Balmer spectra of the Hydrogen atom in a constant magnetic field (for $m^\sigma = 0^+$ final states). Fig. 11(a) shows the raw data, taken at constant scaled energy ϵ as a function of the parameter $\gamma = \text{cte.} \times B$. Proceeding in this way makes it necessary to change the energy E together with the magnetic field B as this latter varies – so that ϵ is constant – but keeps the classical mechanics fixed for the entire spectrum. This raw data seems a priori erratic and featureless. However by performing a frequency analysis (Fourier transform) of these data, well defined peaks emerge, the positions of which identify exactly with the action of the classical closed orbits at the corresponding scaled energy ϵ as expected from the Gutzwiller trace formula.

6.2 Coulomb Blockade in a ballistic quantum dot

Consider next the physics of Coulomb Blockade in ballistic quantum dots. Quantum dots are small puddles of conduction electrons, containing anywhere between a few tens to a few thousand particles. Different kinds of quantum dots exist on the market, but we shall be concerned here more specifically with semiconductor quantum dots (as opposed to metallic ones). Typically, such quantum dots are obtained by patterning a two dimensional electron gas (2DEG) trapped at the interface between (for instance) a Gallium Arsenide (GaAs) and an Aluminum Gallium Arsenide (AlGaAs) compound. Because the impurity donors providing the electrons trapped at the interface can be kept some distance away from the GaAs/AlGaAs interface, such 2DEG's can show very long elastic mean free paths and coherence lengths, in the range of micrometers. Using electrostatic gates or local oxidation of the 2DEG one can build small puddles of electrons within the 2DEG, which are perfectly coherent (in the sense

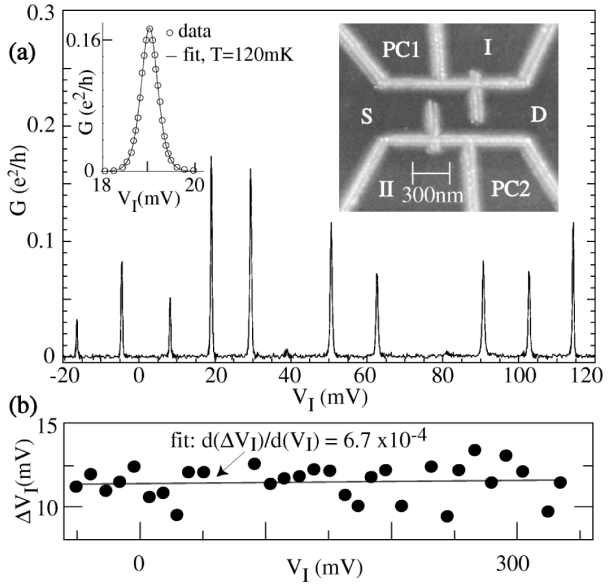


Figure 12: (a) Right inset: Atomic Force Microscopy (AFM) picture of a dot coupled to source (S) and drain (D) through tunnel barriers. Gates *I* and *II* are used to tune the dot electrostatic potential. Main figure: conductance G as a function of V_I , showing Coulomb blockade resonances. Left inset: zoom on a single peak. (b) Spacing between successive peaks. Reprinted figure with permission from [S. Lüscher *et al.*, Phys. Rev. Lett. **86** pp 2118-2121 (2001)]. Copyright (2001) by the American Physical Society.

that their interaction with the outside world does not suppress quantum interference effects) and ballistic (meaning that the effect of disorder associated with impurities can be neglected).

When they are small enough, and at small enough temperature (typically in the sub-Kelvin range), the charging energy, which is the energy scale associated with the electrostatic energy due to the addition of a single electron within the dot, may become significantly larger than the temperature. In this regime, the quantization of the charge becomes important. Indeed, attempting to push a current through the dot by applying a weak voltage between a drain and source connected through tunnel junction to the quantum dot implies having electrons jumping in (from the source) and out (to the drain) from the dot. The energy cost associated with the addition or the removal of an electron is usually too large and that blocks the current flow. This phenomenon is called Coulomb blockade.

When the voltage V_G of a side gate can be tuned however, it can be arranged in such a way that, for a given integer N the energies of the dots with N or $N + 1$ electrons exactly coincide (and correspond to a minimum). For such a value $V_G(N)$ of the gate voltage, a current can then flow through the dot since there is no energy cost to the addition ($N \rightarrow N + 1$) or removal ($N + 1 \rightarrow N$) of an electron. This gives the kind of conductance versus gate voltage dependence illustrated in Fig. 12. As seen in this figure, the Coulomb blockade conductance peaks can be characterized by two quantities that may fluctuate from one peak to the other: their height, and the spacing between two successive peaks.

The former of these fluctuations can be related to those of the wavefunctions at the location of the source and drain contacts. Assuming the motion within the dot is chaotic, and following the same kind of logic that was described in Sect. 5 for spectral statistics, one expects the wavefunction fluctuations to be given by Random Matrix Theory, which implies that they follow a probability density which had come to be known as the Porter-Thomas distribution. From this hypothesis one can derive statistics of peak heights that compare well with experimental

peak high distribution. Understanding the existence of correlations between successive peak heights however requires one to go beyond this simple modeling, and in particular to take into account the role of classical orbits.

Turning now to the peak spacing, we note that the position $V_G(N)$ of the N 'th peak is proportional to the difference $E(N+1) - E(N)$ between the manybody ground state energy of the dot with either N or $N+1$ electrons (and more precisely the “intrinsic” part of that energy, i.e. not including the electrostatic contribution of V_G). The peak spacings are therefore related to the second difference $E(N) + E(N+1) - 2E(N+1)$, implying that the peak spacing fluctuations eventually probe the manybody ground state energy fluctuations.

The simplest possible description of this ground state energy is the constant interaction model, in which only the electrostatic, mean field part, of the Coulomb interaction between electrons is taken into account. Under this approximation the fluctuations are entirely associated with those of the one particle energy levels, which assuming chaotic dynamics, are described by the random matrix ensemble reviewed in Sect. 5. Taking into account the spin degree of freedom, which implies that each one-particle orbital can be occupied twice, this model predicts a clear odd-even effect with a very narrow distribution for odd spacings and Wigner-surmise for even spacings.

The chaotic nature of the dynamics makes it therefore possible to obtain an “universal prediction” for the peak spacing distribution within the constant interaction model, in which the details of the shape of the dots plays little role as long as the dynamics within the dot is chaotic. It turns out that experimentally observed distributions differ significantly from this prediction providing in this way an unambiguous signature of the fundamental role played, beyond the simple mean electrostatic field, by the interactions between electrons. In the resulting Fermi-liquid description the statistical properties of the wavefunctions come into play. Within the semiclassical limit, and using one of the fundamental properties of the random matrix description – namely the invariance under a rotation of the Hilbert space – a “Universal Hamiltonian” description of the dots energy has been obtained which, once higher order terms in this semi-classical development as well as temperature effects are taken into account – together with the experimental issue of “switching events” – give distributions of Coulomb-blockade peak spacing which are in very reasonable agreement with the experimental data for the chaotic dots.

To conclude this subsection, we see that the statistical properties of one-body energy levels as well as eigenfunctions play a fundamental role in the description of the conductance of ballistic quantum dots in the Coulomb Blockade regime. The random matrix description of quantum chaos provides a conceptual framework, as well as a benchmark, for these studies.

6.3 Orbital magnetism of mesoscopic rings or dots

In the early nineties, a few experimental groups were able to measure persistent currents in an ensemble of small metallic rings at sub-Kelvin temperature. These persistent currents are not be confused with the electrical currents that can flow for arbitrary long times in superconductors. Those are, in fact, out of equilibrium phenomenon, whereas the persistent currents are equilibrium properties created by the application of an external magnetic field, and intimately related to the formation of a magnetic moment.

What makes these persistent currents interesting however is that they are a purely quantum effect. A theorem of van Leeuwen states that such persistent currents cannot exist within a classical physics description. Their experimental observation therefore implies that quantum effects, and in particular interference effects, are at work. The metallic rings under study therefore need to be sufficiently small, and at a temperature sufficiently low that they can be considered as perfectly coherent systems.

A theoretical study of these persistent currents, and more generally of the orbital magnetic

response of mesoscopic dots or rings requires taking into account the interactions between electrons, and many issues, some of them presumably related to experimental difficulties, still remains open in this respect. We shall here limit ourself to a model of non-interacting electrons, which is sufficient to capture some features of this magnetic response, such as the typical response of individual systems, but are insufficient for others (such as the mean response for and ensemble of dots or rings).

Working within the grand canonical ensemble, the thermodynamic properties of a system are entirely determined by the knowledge of the thermodynamic potential Ω and its variation with respect to macroscopic variables characterizing the system. For example, if a ring is threaded by a magnetic flux line ϕ , the persistent current is expressed as

$$I_p = -\frac{\partial \Omega}{\partial \phi} . \quad (25)$$

Similarly, the magnetic moment \mathcal{M} of an ensemble of charged particles confined to a spatial region of area A is the derivative with respect to the magnetic field B

$$\mathcal{M} = -\frac{1}{A} \frac{\partial \Omega}{\partial B} . \quad (26)$$

Furthermore, within the model of non-interacting fermions, the grand potential Ω can be expressed entirely in terms of the density of states $d(\epsilon)$ (see Eq. (16))

$$\Omega(T, B, \dots) = -k_B T \int d(E) \log(1 + \exp[(\mu - E)/k_B T]) dE , \quad (27)$$

with T the temperature, μ the chemical potential and k_B the Boltzmann constant.

As discussed in Sect. 4, $d(E)$ can be split into a smooth part $d_W(E)$ and an oscillating one $d^{\text{osc}}(E)$. Quantum interference effects are entirely contained in the contribution from $d^{\text{osc}}(E)$ to Ω . The smooth part $d_W(E)$ on the other hand is associated with a “classical-like” contribution, present even for macroscopic size samples too large for quantum coherence to be preserved. It can be shown, furthermore, that under very general hypotheses $d_W(E)$ has to leading \hbar order no magnetic field dependence. The magnetic response of interest is entirely governed by $d^{\text{osc}}(E)$.

For a chaotic system, inserting the Gutzwiller trace formula Eq. (17) in Eq. (27) implies that the magnetic response of a Fermi gas in the semiclassical limit is entirely determined by the classical trajectories of the analog classical system. Other semiclassical trace formula can be used for other dynamical regimes (e.g. the Berry-Tabor trace formula for integrable dynamics). In addition, the finite temperature sets a time scale $\tau_\beta \stackrel{\text{def}}{=} \hbar/k_B T$ such that the contribution of orbits of period larger than τ_β are averaged out by the thermal fluctuations. For not too low temperatures only the shortest trajectories survive this thermal average, making the enumeration of the orbits relatively straightforward.

One kind of system which has been studied experimentally is weakly disordered rings threaded by a magnetic flux ϕ . For such systems, the microscopic Hamiltonian, and thus the persistent current, has a periodicity $2\pi\phi_0$ in ϕ , with $\phi_0 \stackrel{\text{def}}{=} 2\pi\hbar/e$ the flux quantum, so that the persistent current can be expanded in a Fourier series in ϕ

$$I_p = \sum_n I_n \sin\left(\frac{2\pi n\phi}{\phi_0}\right) . \quad (28)$$

For these weakly disordered rings, the classical motion is diffusive-like which can be seen as a particular type of chaotic motion. Using the Gutzwiller trace formula together with the Hannay-Ozorio sum rule, the latter establishing some connection between the prefactor of the Gutzwiller trace formula and the probability that a particle diffuses back to its starting point,

one obtains that the amplitude I_n has a random sign and magnitude, which depends on the (random) realization of disorder. A typical value $I_{\text{typ}}^{(n)} \stackrel{\text{def}}{=} \langle (I_n^{(n)})^2 \rangle^{1/2}$ has the explicit expression

$$I_{\text{typ}}^{(n)} = \frac{4ne}{\pi} \left[\int_0^\infty \frac{dt}{t^3} R^2(t/t_\beta) \frac{\exp(-n^2 L^2 / 4Dt)}{\sqrt{4\pi Dt / L^2}} \right]^{1/2} \quad (29)$$

with L the circumference of the ring, D the diffusion coefficient $t_\beta \stackrel{\text{def}}{=} \hbar/\pi k_B T$ the characteristic time associated with temperature, and $R(x) \stackrel{\text{def}}{=} \sinh(x)/x$. In spite of its unwelcoming appearance, Eq. (29) has a rather transparent interpretation. The term $P(nL) \stackrel{\text{def}}{=} \exp(-n^2 L^2 / 4Dt) / \sqrt{4\pi Dt}$ is just the probability that an electron diffuses a distance nL , which for a ring of diameter L implies that the particle winds n times around the ring – thus enclosing a flux $n\phi$. The second factor, $R^2(t/t_\beta)$, is then essentially one for $t \ll t_\beta$ and decays exponentially quickly as the time t becomes larger than t_β . It thus plays the role of temperature-dependent cutoff which imposes that the diffusion around the ring should be done in a time shorter than t_β . In the low temperature limit, for which t_β is much larger than the typical time $t_D^{(n)} = (nL)^2 / 4D = n^2 t_D^0$ necessary to diffuse a distance nL , one can perform the integral in Eq. (29) explicitly and obtain

$$I_{\text{typ}}^{(n)} \xrightarrow{T \rightarrow 0} \frac{24\sqrt{5}}{\pi} n^{-3/2} \frac{e}{t_D^0}. \quad (30)$$

As already mentioned, the contribution just discussed has a random sign which varies with the realization of the disorder. This implies that it could be observed for experiments done on a single ring, but not if measurements are performed on a large ensemble of rings. In that case, even within a non-interacting description of the electrons, the fact that the number of electrons rather than the chemical potential is kept fixed as the field is varied gives a contribution I_{av} which is non-vanishing when averaging over disorder realizations. It can be expressed as

$$I_{\text{av}} = \sum_n I_n \sin\left(\frac{4\pi n\phi}{\phi_0}\right), \quad (31)$$

$$I_n = \frac{16\Delta n L}{\phi_0} \int_0^\infty dt \frac{\sinh(t/t_c)}{t^3/t_c^2} \frac{\exp(-n^2 L^2 / 4Dt)}{\sqrt{4\pi Dt}} \quad (32)$$

(note the doubling of frequency in the flux dependence). The physical meaning of the various terms is the same as in Eq. (29). However, as mentioned above, this contribution is presumably dominated by other contributions associated with the interactions between electrons.

Analog calculations can be performed for the magnetization of quantum dots in chaotic as well as integrable geometries. Because of the existence of periodic orbit families, the latter dynamical regime is associated with magnetic response, which for experimentally relevant dot sizes can be order of magnitudes larger than for chaotic systems.

7 Conclusion

Quantum chaos has become a rather broad field, which identifies commonalities between systems of very different type and size and energy scales. It cuts across traditional subject lines that are organized by the nature of the physical system, and contributes understanding through combinations of asymptotic and statistical methods. Beginning from the question of whether there are special properties found in wave mechanical systems (quantum, acoustical, and optical waves) with chaotic counterparts, the field has grown to incorporate some aspects of models on lattices, effective field theories, branches of mathematics, and systems with quantities, such

as spin, that do not have obvious classical analogs. Space limitations did not allow us to cover such extensions, however they are very much a part of the subject and some information can be found in the references given below.

Quantum chaos has developed over the years both in the emergence of new theoretical tools as well as application to and analysis of a wide range of new physical systems. We will not repeat or add to the list of physical applications enumerated in the introduction here, but you will notice the great breadth of physical systems contained in the list. It is worth mentioning or reiterating a few examples where theoretical tools were developed. For semiclassical methods, whereas EBK quantization works only for integrable systems, semiclassical trace formulae were discovered that get past this barrier. Likewise, wave packet propagation in chaotic systems is now understood to be expressible semiclassically as a sum over heteroclinic orbits, those arising in the same orbit tangles discussed by Poincaré more than a hundred years ago for the three-body problem. Previously, one would not have known how to express the dynamics semiclassically. Furthermore, though not mentioned in the text up to this point, there has been an explosion of new kinds of tunneling problems recognized because of the development of new semiclassical methods, chaos-assisted tunneling, resonance-assisted tunneling, chaotic tunneling and ionization, and more. In the department of statistical methods, Wigner's introduction of random matrix theory along with Dyson and Mehta's introduction of new statistical measures gave a whole new way of looking for statistical behaviors. First applied in a strongly interacting many-body context, it was later recognized that the critical element was that if the system's dynamics were chaotic, its statistical properties would be those of random matrix theory.

One important consequence of the theoretical advances that have come from the field of quantum chaos is that it modifies considerably our perception of the Correspondence Principle. In its original formulation, which is found in most quantum mechanics textbooks, this principle is essentially understood as a recipe – roughly speaking, replace Poisson brackets with commutators – to derive the quantum dynamics from a pre-existing classical description. Quantum chaos has shown that the link between classical and quantum dynamics was much more profound and subtle than this. In particular, it has demonstrated that seemingly unrelated points of view, asymptotic methods and statistical analyses, which seem to connect the classical and quantum behavior of a physical system from completely different perspectives, have deep and previously well hidden connections. An important example is the idea that the uniform exploration of phase space by chaotic periodic trajectories weighted by their stability determinants necessarily implies random matrix statistics in the corresponding quantum spectrum. This ability to reveal deep connections between different aspects of a physical system actually goes beyond the realm of the Correspondence Principle. For example, it has also been discovered that random matrix theory emerges from asymptotic analysis applied to effective field theories that were developed for the study of disordered systems. This links random matrix theory or quantum chaos, more generally, to diagrammatic techniques, Anderson localization, and the physics of the metal-insulator transition.

In the course of investigating a specific physical system, quantum chaos is most useful in situations where asymptotic approximations and statistical methods are essential for understanding the physics, but other approaches, such as exact analytic derivations, exact calculations, or perturbation theory, are mostly inadequate. Often a quantum chaotic system behaves at first sight very much like a pseudo-random number generator. There is little information, if any, in a particular eigenvalue of a particular system. Whatever information exists, it is buried either in new statistical laws or in larger scale behavior. Without an understanding of how to extract this information, it is essentially invisible. We gave a few examples in the last section of this review. The study of Coulomb blockade peaks spacing is an illustration of how random matrices provide the basic building blocks for the statistical description of the conductance of quantum dots in the Coulomb blockade regime. On the other hand, for orbital

magnetism semiclassical trace formulas could be used to provide a quantitative understanding of thermodynamic properties of mesoscopic rings or dots. In many other circumstances, both kind of approaches, statistical analysis based on random matrices and semiclassical methods, are used concurrently as was shown for the diamagnetic Hydrogen atom in making sense of an otherwise seemingly inextricable problem.

It was not possible to survey here all the problems for which the concept imported from quantum chaos have been useful. The “supplementary reading” list below will provide some entry points to these studies, as well as to more details accounts of the fundamentals of quantum chaos. A collection of pedagogical articles that fit under the moniker Quantum Chaos can be found in Scholarpedia, url: http://www.scholarpedia.org/article/Category:Quantum_Chaos. We suggest the articles: i) Anderson localization and quantum chaos maps; ii) Chirikov standard map; iii) Quantum baker map iv) Cold atom experiments in quantum chaos; v) Gutzwiller trace formula; vi) Loschmidt echo; vii) Microwave billiards and quantum chaos; and viii) Semiclassical theory of the Helium atom.

Acknowledgments

We are grateful to Amaury Mouchet and Arul Lakshminarayan for their careful reading of the manuscript as well as for their numerous comments and suggestions.

Glossary:

Anderson localization - A classical particle in a disordered medium usually shows a diffusive-like motion. This is also the case for a quantum particle (eg. an electron in a metal) where the disorder is weak (and assuming three dimensional space). For stronger disorder, or smaller dimensions, quantum interference effects make it impossible for the particle to escape some region of space, even for infinite times. This effect is called Anderson localization.

Correspondence principle - Originally, the correspondence principle is the statement that in some limit the quantum behavior of a physical system should be indistinguishable from its classical analogue. This imposes strong constraints on the construction of a quantum operator once the corresponding classical function is known. On the other hand microscopic or mesoscopic objects are – one could say by definition – not in the regime where strictly classical or strictly quantum behavior can be identified. A stronger form of the correspondence principle, which we use here, is that in a larger parameter regime, which includes much of mesoscopic and nano-physics, the classical dynamics strongly influences its quantum counterpart.

Coulomb Blockade - for small quantum dots, the electrostatic energy associated with the addition of a single electron within the dot can become large enough to prevent current from flowing through the dot. This phenomenon is referred to as Coulomb Blockade (as the Coulomb interaction is “blocking” the flow of electrons).

Decoherence - destruction of quantum interferences associated with the interaction with degrees of freedom not explicitly taken into account in the microscopic description of the system under consideration.

Dirac delta function - $\delta(x)$ can be seen as the limit of a function which is zero everywhere except near $x = 0$ keeping the integral $\int \delta(x)dx = 1$.

Disorder - part of a physical system which cannot be controlled experimentally but is on the other hand well modelled by a random description. A typical example in solid state physics would be impurities in an atomic lattice.

Hamiltonian - in classical mechanics a function defined in phase space, and in quantum mechanics an operator acting on the space of wave functions, which corresponds to the energy of the system and governs its time evolution

Husimi function - for a given wavefunction Ψ , its Husimi representation is the function $[\Psi]_H(x, p)$, which to each phase space point $\{(x, p)\}$ associates the value of the overlap between Ψ and a wave packet centered at position x and with mean momentum [velocity] p . The Husimi function $[\Psi]_H(x, p)$ therefore provide a representation in phase space of the wave function Ψ .

Lyapunov exponent - for a chaotic system, the Lyapunov exponent measures the exponential rate of divergence of nearby classical trajectories.

Mesoscopic - larger than microscopic, but smaller than macroscopic. In solid state physics, a mesoscopic system implies more precisely that the system is large enough to contain many (hundred, thousand or more) particles, but is still small enough to be fully coherent (i.e. quantum mechanical) at sufficiently low temperatures.

Orbital magnetism - magnetic response of an ensemble of electrons associated with the coupling of the magnetic field with the orbital motion of the electrons. Orbital magnetism is a thermodynamic (i.e. equilibrium) effect.

Operator - an operator is an object that acts linearly on a space of functions (such as the quantum wave functions). As this space of functions is a vector space of infinite dimension, an operator can be seen simply as a matrix of infinite dimension.

Phase space - space in which both the position x and momentum p of a classical particle (or system) is represented.

Quantum dots (disordered and ballistic) - Quantum dots are small puddles of electrons, on the micrometer or nanometer scale. Example of quantum dots are : i) small metallic grains, which usually are disordered (as impurities or lattice defects are always present in the metal); ii) semiconductor quantum dots obtained by patterning two dimensional electron gasses (formed at the interface between two semiconductors) with electrostatic gates. In some circumstances these semiconductor quantum dots can be made clean (i.e. defect free) enough that electrons can be considered to move ballistically (i.e. as in free space) in the interior of the quantum dot.

Quantum entanglement - intertwining of two (or more) quantum subsystems through quantum superposition.

Quantum information theory - Information theory is based on the utilization of quantum qubits. Qubits are essentially two-level systems and represent the quantum version of the classical bits (logical units with value 0 or 1).

Quantum tunneling - Because of its wave character, a quantum particle can have a finite probability to traverse a potential energy barrier higher than its total energy, and more generally to move to a location which is impossible to reach through classical motion. This phenomenon is referred to as quantum tunneling.

Stadium billiard - billiard system with the shape of a stadium, namely two straight parallel sides joined with two semi-circles, i.e. the shape of a hippodrome.

Torus - in its simplest form, a 2-dimensional torus can be seen as a rectangle for which opposite sides have been identified so as to create a periodicity, i.e. exiting to the right implies entering from the left. Any 2-dimensional manifold which can be mapped continuously on this basic torus will be also considered as a torus. This notion can be generalized straightforwardly to any dimension $d \geq 1$ (eg. a one dimensional torus is just a circle). For integrable (or near integrable) classical motion, it can be shown that the regular trajectories are trapped on invariant manifold with the topology of tori.

Trace of a matrix or of an operator - the trace of a matrix, or of an operator is just the sum of its diagonal elements.

Further reading:

- [1] M. J. Giannoni, A. Voros, and J. Jinn-Justin, editors. *Chaos and Quantum Physics*. North-Holland, Amsterdam, 1991; [contains several introductory courses that together comprise the main foundations of quantum chaos].
- [2] C. E. Porter. *Statistical Theories of Spectra: Fluctuations*. Academic Press, New York, 1965; [begins with a readable overview of random matrix theory and contains a collection of its early foundational research papers].
- [3] M. L. Mehta. *Random Matrices (Third Edition)*. Elsevier, Amsterdam, 2004; [explains mathematical methods used to derive many of the important results coming from early random matrix theory].
- [4] H.-J. Stöckmann. *Quantum Chaos: An Introduction*. Cambridge University Press, New York, 1999; [a pedagogical introduction to random matrix theory].
- [5] M. C. Gutzwiller. *Chaos in Classical and Quantum Mechanics*. Springer-Verlag, New York, 1990; [covers the basic semiclassical theory that relates properties of periodic orbits to quantum spectra, and is known loosely as periodic orbit theory].
- [6] A. M. Ozorio de Almeida. *Hamiltonian systems: Chaos and quantization*. Cambridge University Press, Cambridge, 1988; [contains many sophisticated results in classical mechanics that become very useful in semiclassical theory for understanding quantum statistics, symmetry breaking, and the relations with random matrix theory].
- [7] P. Cvitanović, R. Artuso, R. Mainieri, G. Tanner and G. Vattay, *Chaos: Classical and Quantum*, ChaosBook.org Niels Bohr Institute, Copenhagen 2012; [very complete Web-Book – with links to online courses and videos – with a special focus on classical and quantum trace formulae].
- [8] V. P. Maslov and M. V. Fedoriuk. *Semiclassical approximation in quantum mechanics*. Reidel Publishing, Dordrecht, 1981; [gives a rigorous mathematical treatment of stationary phase and saddle point approximations that generate semiclassical theory, which relates classical and quantum mechanics].
- [9] E. J. Heller and S. Tomsovic. Post-modern quantum mechanics. *Physics Today* 46(7):38–46, 1993; [reviews semiclassical theory starting with time dependent quantum mechanics and wave packets].

- [10] O. Bohigas, S. Tomsovic, and D. Ullmo. Manifestations of classical phase space structures in quantum mechanics. *Phys. Rep.*, 223:43–133, 1993; [explains how classical structures, i.e. tori and chaotic transport barriers, give rise to new quantum phenomena such as modified spectral statistics, chaos-assisted tunneling, and eigenfunction localization].
- [11] D. Braun. *Dissipative quantum chaos and decoherence*. Springer, Berlin, 2001; [one of the few accounts of how to incorporate decoherence and dissipation into the subject of quantum chaos].
- [12] S. Keshavamurthy and P. Schlagheck, editors. *Dynamical Tunneling: Theory and Experiment*. CRC Press, Boca Raton, 2011; [contains several contributions that describes many new features of quantum tunneling discovered in the past twenty years. Typically, the new phenomena can be related to the presence of chaos in the classical dynamics].
- [13] H. Friedrich and D. Wintgen. The Hydrogen atom in a uniform magnetic field – an example of chaos. *Phys Rep*, 183:37–79, 1989; [contains a comprehensive treatment of the diamagnetic Hydrogen atom as a physical realization of a quantum chaotic system].
- [14] T. A. Brody, J. Flores, J. B. French, P. A. Mello, A. Pandey, and S. S. M. Wong. Random-matrix physics: spectrum and strength fluctuations. *Rev. Mod. Phys.*, 53:385–479, 1981; [reviews the foundations of random matrix theory especially in the context of statistical nuclear physics].
- [15] O. Bohigas and H. A. Weidenmueller. Aspects of chaos in nuclear physics. *Ann. Rev. Nucl. Part. Sci.*, 38:421–453, 1988; [a review of how random matrix theory enters statistical nuclear physics with attention given to scattering formulations].
- [16] Fritz Haake. *Quantum Signatures of Chaos* Springer-Verlag, Berlin Heidelberg, 2010 (third edition); [general overview about quantum chaos, includes some discussion of supersymmetric techniques].
- [17] P. Leboeuf. *Regularity and Chaos in the Nuclear Masses*. Lecture Notes in Physics 652, Springer, Berlin Heidelberg, 2005; [discusses the role of periodic orbits and chaotic dynamics in nuclear masses]
- [18] C. W. J. Beenakker. Random-matrix theory of quantum transport. *Rev. Mod. Phys.*, 69(3):731–808, 1997; [contains a review of how random matrix theory is used to describe mesoscopic electrical conductors].
- [19] D. Ullmo. Many-body physics and quantum chaos. *Rep. Prog. Phys.*, 71:026001, 2008; [reviews the many ways that quantum chaos, both semiclassical theory and random matrix methods, enter into many-body problems especially in the context of mesoscopic physics].
- [20] Y. Imry. *Introduction to Mesoscopic Physics*. Oxford University Press, 1997; [provides a general introduction to electronic mesoscopic systems].
- [21] K. Richter. *Semiclassical Theory of Mesoscopic Systems*. Springer-Verlag, 2000; [describes how the semiclassical techniques developed in the field of quantum chaos can be used to understand physical properties of mesoscopic systems].
- [22] E. Akkermans and G. Montambaux. *Mesoscopic Physics of Electrons and Photons*. Cambridge University Press, 2007; [contains a readable and rigorous description of our understanding of the physical properties of mesoscopic systems].

- [23] I. L. Aleiner, P. W. Brouwer, and L. I. Glazman. Quantum effects in coulomb blockade. *Phys. Rep.*, 358:309–440, 2002; [reviews the phenomenon of Coulomb Blockade in mesoscopic dots in the low temperature regime where quantum effects are relevant].
- [24] K. Richter, D. Ullmo, and R. A. Jalabert. Orbital magnetism in the ballistic regime: geometrical effects. *Phys. Rep.*, 276:1, 1996; [gives the theory of the response of mesoscopic conductors to the application of magnetic fields].
- [25] M. Wright and R. Weaver, editors. *New directions in linear acoustics and vibration: quantum chaos, random matrix theory and complexity*. Cambridge, 2010; [a collection of introductory courses detailing how quantum chaos (semiclassical theory and random matrix theory) enters into various acoustic problems].

Biographical sketch

Denis Ullmo

Denis Ullmo earned a Ph.D. in theoretical physics from the university of Paris-Sud in 1992 under the direction of Oriol Bohigas. He then worked within the Theoretical Division of the Nuclear Physics Institute of Orsay until he was appointed resident visitor at the Bell Laboratories (Murray Hill, NJ) from December 1994 to May 1997. After this, he joined the LPTMS (Laboratoire de Physique Thorique et Modèles Statistiques, Paris-Sud university) where he now holds a Directeur de Recherche position at the French CNRS (Centre National de Recherche Scientifique). During that period, he spent three years (from 2002 to 2005) as a visiting professor at Duke University (North Carolina) in the group of Harold Baranger.

Denis Ullmo's scientific interests include quantum chaos and its applications to mesoscopic physics. He has worked in particular on quantum tunneling in the presence of chaos, as well as on the thermodynamic and transport properties of quantum dots.

Steven Tomsovic

Steve Tomsovic earned a Ph.D. in theoretical and statistical nuclear physics from the University of Rochester in 1987 with J. B. French. Afterward he received a Joliot-Curie Fellowship and IN2P3 stipend to work with Oriol Bohigas in Orsay, France for two years. He then spent six years working with Eric Heller at the University of Washington, one year of which was spent visiting the Harvard-Smitsonian Center for Astrophysics as a Fellow. Now a professor at Washington State University, he was department chair of Physics and Astronomy for eight years. He has been an invited visiting professor at the *Laboratory for Theoretical Physics and Statistical Models* in Orsay, France, and at the *Indian Institute for Technology Madras* in Chennai, India, and was also recently awarded a *Senior Research Fulbright Fellowship* for work in Germany, and held the *Martin Gutzwiller Fellowship* of the *Max Planck Institute for the Physics of Complex Systems* in Dresden, Germany. He has organized a number of international programs and conferences.

Steven Tomsovic research specialties include the wave mechanics of chaos and disorder, semiclassical methods, random matrix theory, statistical nuclear physics, mesoscopic systems, and long range ocean acoustics.